

VLT SPECTROSCOPY OF BLUE SUPERGIANTS IN IC 1613<sup>1</sup>

FABIO BRESOLIN AND MIGUEL A. URBANEJA

Institute for Astronomy, 2680 Woodlawn Drive, Honolulu, HI 96822;  
bresolin@ifa.hawaii.edu, urbaneja@ifa.hawaii.edu

AND

WOLFGANG GIEREN AND GRZEGORZ PIETRZYŃSKI

Universidad de Concepción, Departamento de Física, Casilla 160-C, Concepción, Chile;  
wgieren@astro-udec.cl, pietrzn@hubble.cfm.udec.cl

AND

ROLF-PETER KUDRITZKI

Institute for Astronomy, 2680 Woodlawn Drive, Honolulu, HI 96822;  
kud@ifa.hawaii.edu

## ABSTRACT

We present multi-object spectroscopy of young, massive stars in the Local Group galaxy IC 1613. We provide the spectral classification and a detailed spectral catalog for 54 OBA stars in this galaxy. The majority of the photometrically selected sample is composed of B- and A-type supergiants. The remaining stars include early O-type dwarfs and the only Wolf-Rayet star known in this galaxy. Among the early B stars we have serendipitously uncovered 6 Be stars, the largest spectroscopically confirmed sample of this class of objects beyond the Magellanic Clouds. We measure chemical abundances for 9 early-B supergiants, and find a mean oxygen abundance of  $12 + \log(\text{O}/\text{H}) = 7.90 \pm 0.08$ . This value is consistent with the result we obtain for two H II regions in which we detect the temperature-sensitive [O III]  $\lambda 4363$  auroral line.

*Subject headings:* galaxies: abundances — galaxies: stellar content — galaxies: individual (IC 1613) — stars: early-type

## 1. INTRODUCTION

IC 1613 is a Local Group dwarf irregular galaxy, member of the M31 subgroup (McConnachie & Irwin 2006), located at a distance of  $721 \pm 12$  kpc (Pietrzyński et al. 2006). Its low metal content has been derived both from the photometry of the intermediate-age population of stars ( $[\text{Fe}/\text{H}] \simeq -1.3$ ; Cole et al. 1999, Rizzi et al. 2007) and from H II region spectra [ $12 + \log(\text{O}/\text{H}) \simeq 7.70$ ; Kingsburgh & Barlow 1995, Lee et al. 2003].

The evolved stellar populations of IC 1613 have been examined in detail from Hubble Space Telescope imaging programs. The star formation rate in an outlying field 1.6 kpc in projection from the galactic center was shown by Skillman et al. (2003) to have peaked between 3 and 6 Gyr ago, and during the last Gyr it has been suppressed if compared to the central field studied by Cole et al. (1999). The ongoing star formation activity is concentrated in an off-center region,  $\sim 1$  kpc to the north-east of the geometrical center of IC 1613, in correspondence of the peak of the H I distribution (Lake & Skillman 1989) and of the largest concentration of H II region complexes (Hodge et al. 1990), giant ionized shells (Meaburn et al. 1988), young stars (Hodge et al. 1991) and OB associations (Hodge 1978; Borissova et al. 2004).

The young stellar content of IC 1613 has been investigated by Sandage & Katem (1976), Freedman (1988) and Georgiev et al. (1999), among others. More recently, Valdez-Gutiérrez et al. (2001) and Lozinskaya et al. (2003) have examined the interplay between young stars and the kinematics of the neutral and ionized gas, and the effects of stellar winds and supernova explosions on the structure and energy balance of the ISM. The presence of numerous OB

associations appears to provide sufficient mechanical energy to explain the observed expansion of most of the superbubbles within the standard framework of Weaver et al. (1977). However, Silich et al. (2006) find that the multiple winds and supernovae model is not consistent with the observed mass and dimensions of the largest, kpc-size H I supershell. The incomplete characterization of the massive stellar population, in particular with regard to the spectral types of the OB stars that ionize the gas and that blow their stellar winds into the interstellar medium, are major limitations for these studies on the links between young stars and gas in this galaxy.

Previous spectroscopic work on the stellar content of IC 1613 has focused on the search for Wolf-Rayet (W-R) stars and other emission-line objects (Lequeux et al. 1987, Azzopardi et al. 1988, Armandroff & Massey 1991). The high-excitation WO3 star in the H II region S3 (Sandage 1971), in particular, has received a great deal of attention since its discovery (D’Odorico & Rosa 1982, Davidson & Kinman 1982, Garnett et al. 1991, Kingsburgh & Barlow 1995), and remains the only confirmed W-R star in this galaxy. In addition to the early work by Humphreys (1980), who obtained spectra of 7 of the brightest BA and M supergiants with the Kitt Peak 4m telescope, the spectroscopy of a dozen stars in the NE quadrant of IC 1613 obtained with the Special Astrophysical Observatory 6m telescope has been published by Lozinskaya et al. (2002). However, the quality of these spectra is only adequate for a preliminary spectral classification.

In this paper we present 3–5 Å resolution spectra of 54 OBA stars in IC 1613 brighter than  $V = 20.2$ , obtained with the European Southern Observatory (ESO) Very Large Telescope (VLT) in the context of the Araucaria Project (Gieren et al. 2005). This work follows similar spectroscopic work recently carried out by our group on blue supergiants in the galaxies

<sup>1</sup> Based on VLT observations for ESO Large Programme 171.D-0004.

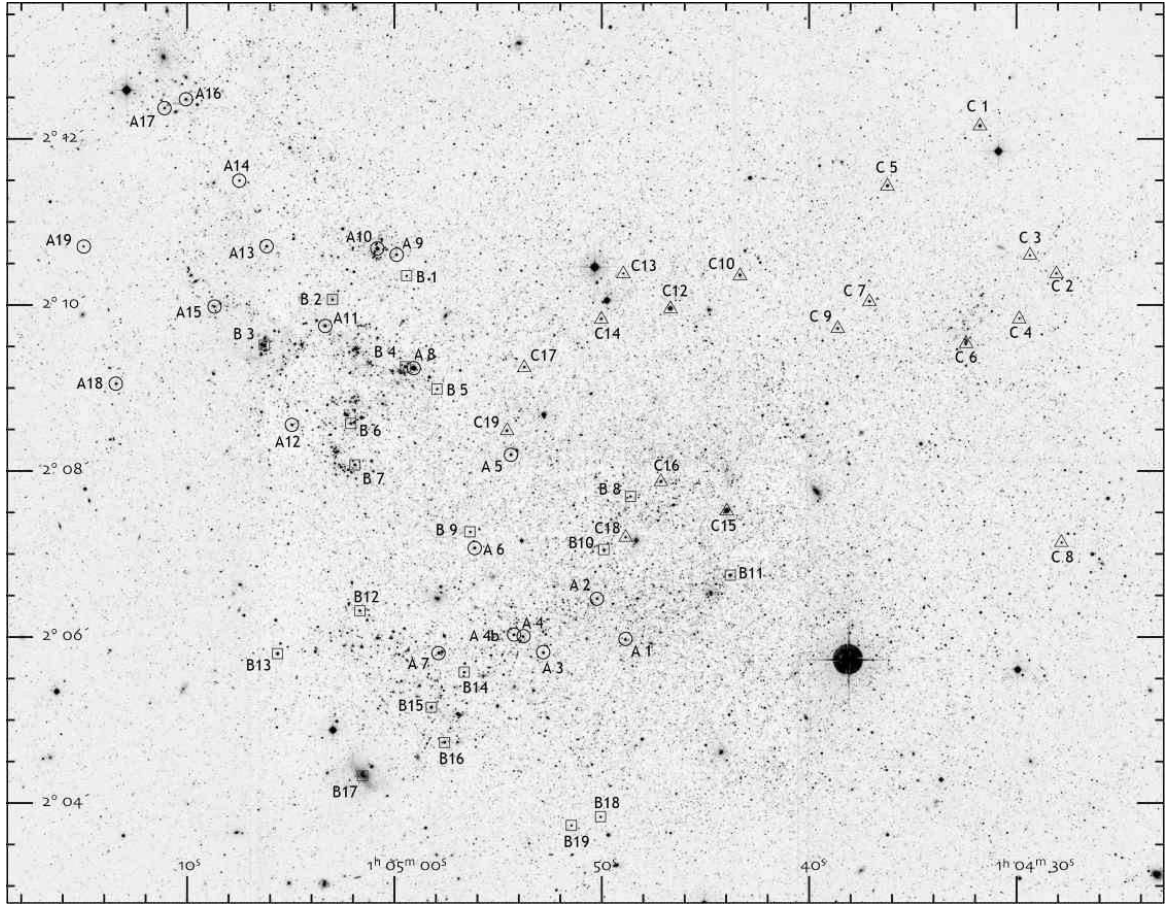


FIG. 1.— Finding chart for the spectroscopic targets. Different symbols are used for stars in fields A (circles), B (squares) and C (triangles). The image has been obtained with a Sloan  $g$  filter at the MegaPrime imager at the CFHT telescope on Mauna Kea. North is up and east is to the left. (courtesy L. Rizzi and B. Tully)

NGC 300 (Bresolin et al. 2002), WLM (Bresolin et al. 2006) and NGC 3109 (Evans et al. 2007). One main motivation for this paper is to present a catalog of spectra and a classification of spectral types for the observed targets. This will be useful for future spectroscopic investigations of the blue supergiants in IC 1613 at higher spectral resolution. Moreover, we carry out the first determination of the chemical abundances of blue supergiants in this galaxy, by fitting model spectra to the data obtained for 9 early B-type stars. The paper is organized as follows: in §2 we describe the observations and the data reduction, and in §3 we present the spectral catalog. In §4 and §5 we discuss the chemical abundances measured in B-type stars and H II regions, respectively. We conclude with a summary in §6.

## 2. OBSERVATIONS

Blue supergiant candidates were selected from  $VI$  photometry measured on images obtained with the Warsaw 1.3m telescope at Las Campanas as part of the OGLE-II collaboration by Udalski et al. (2001). The spectroscopy was carried out at the VLT UT4 (Yepun), equipped with the Focal Reducer and Low Dispersion Spectrograph 2 (FOR2), on the nights of October 26 and 27, 2003. Seeing conditions were variable between  $0''.8$  and  $1''.3$ .

We acquired spectra in three  $6''.8 \times 6''.8$  FOR2 fields in the movable slitlets (MOS) mode (19 slitlets per field, each 1 arcsec wide and extending  $\sim 21$  arcsec in the spatial direction). We included as many of the brightest blue stars ( $V < 20$ ,  $V - I < 0.4$ ) found in the three fields of IC 1613 as possible.

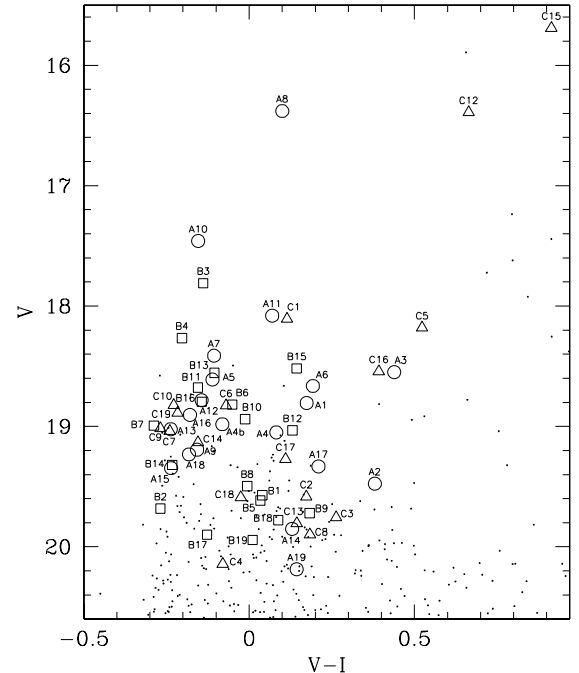


FIG. 2.— Location of the spectroscopic targets in the  $V$  vs.  $V - I$  color-magnitude diagram. Different symbols are used for stars in fields A (circles), B (squares) and C (triangles).

A handful of redder or fainter stars were also observed, in order to fill up the MOS setup. A finding chart is shown in

TABLE 1  
IC 1613 - SPECTROSCOPIC TARGETS

Slit Number (1)	R. A. (J2000.0) (2)	Decl. (J2000.0) (3)	V (4)	V - I (5)	Spectral Type (6)	K/(H + He) (7)	$W_\gamma$ (Å) (8)	S/N (9)	$V_{\text{Helio}}$ (km s <sup>-1</sup> ) (10)	Comments <sup>a</sup> (11)
Field A										
1.....	1 04 48.89	2 05 59.5	18.81	0.17	A0 II	0.27	5.4	74	-229	SK E33
2.....	1 04 50.26	2 06 29.2	19.48	0.38	A5 II	0.81	6.8	54	-214	SK E42
3.....	1 04 52.87	2 05 50.1	18.55	0.44	A7-F0 Ib	0.95	5.4	77	-235	SK F33
4.....	1 04 53.84	2 06 01.9	19.05	0.08	B9 II	0.14	4.7	68	-225	SK 23a
4b.....	1 04 54.29	2 06 03.1	18.98	-0.08	B5 Ib	0.20	3.1	52	-276	SK 23A
5.....	1 04 54.41	2 08 13.7	18.61	-0.11	B3 Ib	0.13	2.6	87	-230	
6.....	1 04 56.17	2 07 06.1	18.66	0.19	A3 II	0.59	6.4	81	-228	
7.....	1 04 57.92	2 05 49.9	18.41	-0.11	B2 Iab	0.13	2.2	96	-250	
8.....	1 04 59.06	2 09 17.0	16.38	0.10	A2 Ia	0.44	0.41	235	-241	III SK A43
9.....	1 04 59.94	2 10 38.6	19.19	-0.16	B5 Iab	0.17	2.6	72	-223	III SK 22c
10.....	1 05 00.87	2 10 43.0	17.46	-0.15	B1 Ia	0.20	1.4	159	-255	III SK 22A
11.....	1 05 03.39	2 09 47.2	18.08	0.07	B9 Ia	0.30	1.7	110	-241	III
12.....	1 05 04.99	2 08 35.4	18.78	-0.14	B1.5 Iab	0.17	2.1	89	-226	III SK C52
13.....	1 05 06.21	2 10 44.8	19.02	-0.24	O3-O4 V((f))	0.23	2.2	82	-240	III SK 22b
14.....	1 05 07.51	2 11 32.4	19.85	0.13	Be	< 0.25	in em.	52	-210	
15.....	1 05 08.74	2 10 01.1	19.35	-0.24	O9.5 III	0.32	1.7	74	-279	III
16.....	1 05 10.10	2 12 31.3	18.90	-0.18	early B Ib	...	2.9	86	-233	
17.....	1 05 11.13	2 12 25.0	19.33	0.21	Be	...	in em.	65	-195	
18.....	1 05 13.50	2 09 05.3	19.23	-0.18	B1 Iab	0.17	2.3	70	-229	III
19.....	1 05 15.05	2 10 45.0	20.19	0.14	Be	0.73	in em.	43	-206	
Field B										
1.....	1 04 59.44	2 10 23.2	19.57	0.04	B9 II	0.23	6.3	60	-253	III SK A19
2.....	1 05 03.03	2 10 06.1	19.68	-0.27	O5-O6 V	0.34	1.2	66	-229	III S17 <sup>b</sup>
3.....	1 05 06.34	2 09 32.9	17.81	-0.14	B0 Ia	0.12	1.4	154	-250	III SK B42
4.....	1 04 59.52	2 09 17.6	18.27	-0.20	B1.5 Ia	0.19	1.8	114	-243	III SK A42
5.....	1 04 57.98	2 09 01.2	19.61	0.03	Be	...	in em.	57	-257	III SK 32b
6.....	1 05 02.16	2 08 36.5	18.82	-0.05	B1 Ia	0.19	1.5	92	-268	III SK 38a
7.....	1 05 01.95	2 08 06.5	18.99	-0.29	O9 I	0.14	2.2	87	-241	III SK 38b
8.....	1 04 48.63	2 07 43.3	19.50	-0.01	B8 Ib	0.10	3.6	63	-249	SK D31
9.....	1 04 56.38	2 07 17.8	19.72	0.18	A3 II	0.57	7.7	53	-232	
10.....	1 04 49.93	2 07 04.7	18.94	-0.01	B8 Iab	0.10	3.3	84	-236	SK E46
11.....	1 04 43.82	2 06 46.1	18.68	-0.16	O9.5 I	0.23	2.2	93	-257	III SK L
12.....	1 05 01.72	2 06 20.7	19.03	0.13	Be	...	in em.	80	-225	SK J46
13.....	1 05 05.70	2 05 49.6	18.56	-0.10	B5 Iab	0.15	2.2	98	-221	SK PeM
14.....	1 04 56.69	2 05 36.0	19.32	-0.23	B0 Iab	0.08	2.2	74	-228	SK H33
15.....	1 04 58.28	2 05 10.5	18.52	0.14	A0 II	0.31	5.6	98	-267	III SK H34
16.....	1 04 57.64	2 04 45.2	18.80	-0.14	B1.5 Iab	0.18	2.3	91	-242	III SK H8
17.....	1 05 01.62	2 04 21.1	19.90	-0.13	WO3	...	in em.	47	-245	III DR1 <sup>c</sup> S3 <sup>b</sup>
18.....	1 04 50.11	2 03 51.0	19.78	0.09	B9 II	0.11	5.5	51	-250	
19.....	1 04 51.52	2 03 44.8	19.94	0.01	Be	0.37	in em.	47	-245	
Field C										
1.....	1 04 31.75	2 12 11.1	18.11	0.11	A2 II	0.34	6.1	72	-269	
2.....	1 04 28.07	2 10 24.0	19.58	0.17	A3 II	0.61	7.0	35	-254	
3.....	1 04 29.35	2 10 37.0	19.76	0.26	A3 II	0.71	7.5	31	-259	
4.....	1 04 29.87	2 09 51.5	20.14	-0.08	B8 II	0.15	4.7	28	-249	
5.....	1 04 36.22	2 11 27.7	18.18	0.52	A V	0.81	3.2	57	17	
6.....	1 04 32.45	2 09 33.1	18.83	-0.07	B1 Ia	0.22	1.5	57	-245	III
7.....	1 04 37.09	2 10 04.0	19.04	-0.24	B1 Ia	0.20	1.9	48	-262	
8.....	1 04 27.84	2 07 09.2	19.90	0.18	A3 II	0.62	7.8	30	-232	
9.....	1 04 38.63	2 09 44.4	19.02	-0.27	O8 III((f))	0.18	2.0	52	-258	
10.....	1 04 43.35	2 10 23.4	18.82	-0.23	B1.5 Ib	0.21	2.7	56	-272	
12.....	1 04 46.71	2 09 59.4	16.39	0.66	G2	1.03	2.3	130	-96	
13.....	1 04 48.98	2 10 24.8	19.80	0.14	early A II	...	8.2	32	-227	
14.....	1 04 50.05	2 09 51.8	19.13	-0.16	B2 Ib	...	2.5	47	-232	
15.....	1 04 43.99	2 07 33.0	15.69	0.91	G8	1.00	2.1	156	-78	SK D51
16.....	1 04 47.17	2 07 54.2	18.54	0.39	A5 Ib	0.82	5.9	55	-236	III SK D22
17.....	1 04 53.76	2 09 17.1	19.27	0.11	early A II	...	7.1	43	-239	
18.....	1 04 48.88	2 07 13.8	19.59	-0.02	B5 II	0.09	3.7	37	-224	SK D28
19.....	1 04 54.61	2 08 31.1	18.89	-0.22	composite	0.26	1.7	55	-240	

NOTE. — Units of right ascension are hours, minutes, and seconds, and units of declination are degrees, arcminutes, and arcseconds.

<sup>a</sup> SK numbers from Sandage & Katem (1976). The presence of nebular lines contaminating the stellar spectra is noted with III. <sup>b</sup> H II regions from Sandage (1971). <sup>c</sup> W-R star discovered by D'Odorico & Rosa (1982).

TABLE 2  
OBSERVING LOG

Field	Center (J2000.0)		Grism	Date	Exposure Time (s)
	R. A.	Decl.			
A...	01 05 01.6	02 09 02	600B	10-26-2003	3×2400
			1200R	10-26-2003	3×2700
B...	01 04 57.1	02 07 08	600B	10-27-2003	3×2700
			1200R	10-27-2003	3×2700
C...	01 04 38.9	02 09 07	600B	10-26-2003	2×1800, 1×700
			1200R	10-27-2003	2×1200, 1×1800

Fig. 1, while target coordinates, photometric measurements and other derived parameters are presented in Table 1. Fig. 2 shows the location of the spectroscopic targets in the color-magnitude diagram. Throughout this paper we adopt the convention of appending the slit number (1 to 19) to the field identification (A, B or C) to label our spectroscopic targets. Our field A is centered on the NE quadrant of IC 1613, where the majority of the young stars and H II regions are located. Field B covers most of the central bar-like structure that runs from the SE to the NW, while field C extends to the west of these two main structures. Two stars were included in the 4th slitlet of field A, and are labeled as A4 and A4b. Star C11 was too close to the slitlet edge to provide a meaningful extraction, and therefore it does not appear in Table 1.

The spectroscopy was carried out using two different grisms: the 600B to cover the blue wavelengths (in particular the 3600-5000 Å range, which is critical for the spectral classification) at 5 Å resolution, and the 1200R to cover the region around the H $\alpha$  line at 3 Å resolution. The integration times varied among the different fields and setups, and are summarized in Table 2. As field C contained our lowest-priority targets, the exposure times were shorter than in the remaining two fields. The airmass of IC 1613 was also larger during the spectroscopy of field C, exceeding a value of 1.6. For fields A and B the airmass varied between 1.1 and 1.5.

We have used standard long-slit spectroscopy tasks within IRAF<sup>2</sup> for bias and flat-field corrections, wavelength calibration and extraction of the spectra. Cosmic rays were removed with the L.A.COSMIC routines by van Dokkum (2001). The mean signal-to-noise ratio (S/N) of the resulting averaged, normalized spectra is reported in column 9 of Table 1. The heliocentric radial velocities measured from the spectral lines (column 10) are in all cases but 3 in good agreement with the H I systemic velocity of  $-234 \pm 1$  km s<sup>-1</sup> (Lu et al. 1993). Excluding stars C12 and C15 (2 foreground G stars) and C5 (presumably a Galactic halo A star), we obtain a mean radial velocity of  $-241 \pm 18$  km s<sup>-1</sup>. With an uncertainty of  $\sim 10$  km s<sup>-1</sup> on the radial velocities, and a maximum rotational velocity of  $\sim 20$  km s<sup>-1</sup> from H I observations (Lake & Skillman 1989, Hoffman et al. 1996), we are finding no hints of galactic rotation from our stellar data.

Cross identification with the bright star catalog of Sandage & Katem (1976) is given in column 11 of Table 1. We also indicate the presence of spatially extended nebular emission superposed on the stellar spectra. In some cases this contamination strongly affects the stellar lines, in particular those of the Balmer series.

<sup>2</sup> IRAF is distributed by the National Optical Astronomy Observatories, which are operated by the Association of Universities for Research in Astronomy, Inc., under cooperative agreement with the National Science Foundation.

### 3. SPECTRAL CATALOG

The philosophy behind the classification of extragalactic early-type stars has been discussed at length in our previous works on WLM (Bresolin et al. 2006) and NGC 3109 (Evans et al. 2007). We recall here that for B stars we follow Lennon (1997), and for A supergiants we adopt the criteria from Evans & Howarth (2003) and Evans et al. (2004). The classification of O stars is based upon Walborn (1971), Walborn & Fitzpatrick (1990) and Walborn et al. (2000). Luminosity classes for B and A stars are determined from the equivalent width of H $\gamma$  ( $W_\gamma$ ), following the criteria by Azzopardi (1987).

The spectral classification of the 57 stars included in this work are given in column 6 of Table 1, together with the Ca II K/(Ca II H + H $\epsilon$ ) ratio used for classifying A stars (column 7) and  $W_\gamma$  (column 8). The blue region (3750 Å to 5000 Å) of the normalized stellar spectra is shown in Fig. 3–8, in order of decreasing temperature (spectral type O to G). Emission-line stars are shown in Fig. 9 and 10. In these figures we identify the main H, He and metal lines that are used in the classification procedure.

#### 3.1. Comments on selected stars

We provide here brief comments on some peculiar or outstanding stars presented in Table 1 and shown in Figures 3–10. Absolute magnitudes are derived from a distance modulus  $(m-M)_0 = 24.291 \pm 0.035$  and  $E(B-V) = 0.090 \pm 0.019$  (Pietrzyński et al. 2006).

A8 (A2 Ia).—This is the visually brightest star in IC 1613 at  $M_V = -8.2$ . Sandage & Katem (1976) suggested that this star (their A43) is a foreground field star, but its radial velocity was found to agree with the systemic velocity by Humphreys (1980), who assigned a A0 Ia spectral type. The H $\alpha$  (not shown) and H $\beta$  lines are in emission, with P Cygni profiles. The other non-Be stars with strong wind emission in H $\alpha$  are the B1 supergiants B6 and C6.

A10 (B1 Ia).—Star 22A in the list of Sandage & Katem (1976), it was found by these authors to be the brightest blue star in IC 1613 ( $M_V = -7.1$ ). Humphreys (1980) classified this star as B2-B3 I. We assign the earlier B1 type, from the detection of Si IV  $\lambda\lambda 4089, 4116$  (the latter line blended with He I  $\lambda 4121$ ), and the lack of He II lines.

A13 (O3-O4 V(f)).—The earliest star in our sample shows no evidence of He I in its spectrum, except perhaps a weak He I  $\lambda 4471$  line. Since nebular lines (e.g. [O III]  $\lambda 5007$ ) are present in our spectrum, this lack of He I lines could be due to line in-filling. The strong He II  $\lambda 4686$  absorption and the weak N III  $\lambda\lambda 4634-4640-4642$  emission lines lead to the ((f)) classification. A weak N IV  $\lambda 4058$  in emission is detected. The absolute magnitude of this star,  $M_V = -5.5$ , is consistent with the dwarf classification (Conti 1988).

B2 (O5-O6 V).—This O star displays He I lines in its spectrum, with He II  $\lambda 4200 >$  He I  $\lambda 4026$  (the two lines are of equal strength at class O6). Its value of  $\log W' = \log W(\text{He I } \lambda 4471) - \log W(\text{He II } \lambda 4542) = -0.42$  corresponds to an O5.5 type (Conti 1988). This star is the likely ionizing source of the surrounding H II region S17 (Sandage 1971), whose chemical abundance is derived in Section 5. The contamination by the nebular lines is causing in-filling of the He I lines, therefore the spectral type can be somewhat later than O5-O6. From the H $\alpha$  luminosity of S17 published by Hodge et al. (1990),  $\log L(\text{H}\alpha) = 36.96$  erg s<sup>-1</sup>, we derive the number of Lyman continuum ionizing photons

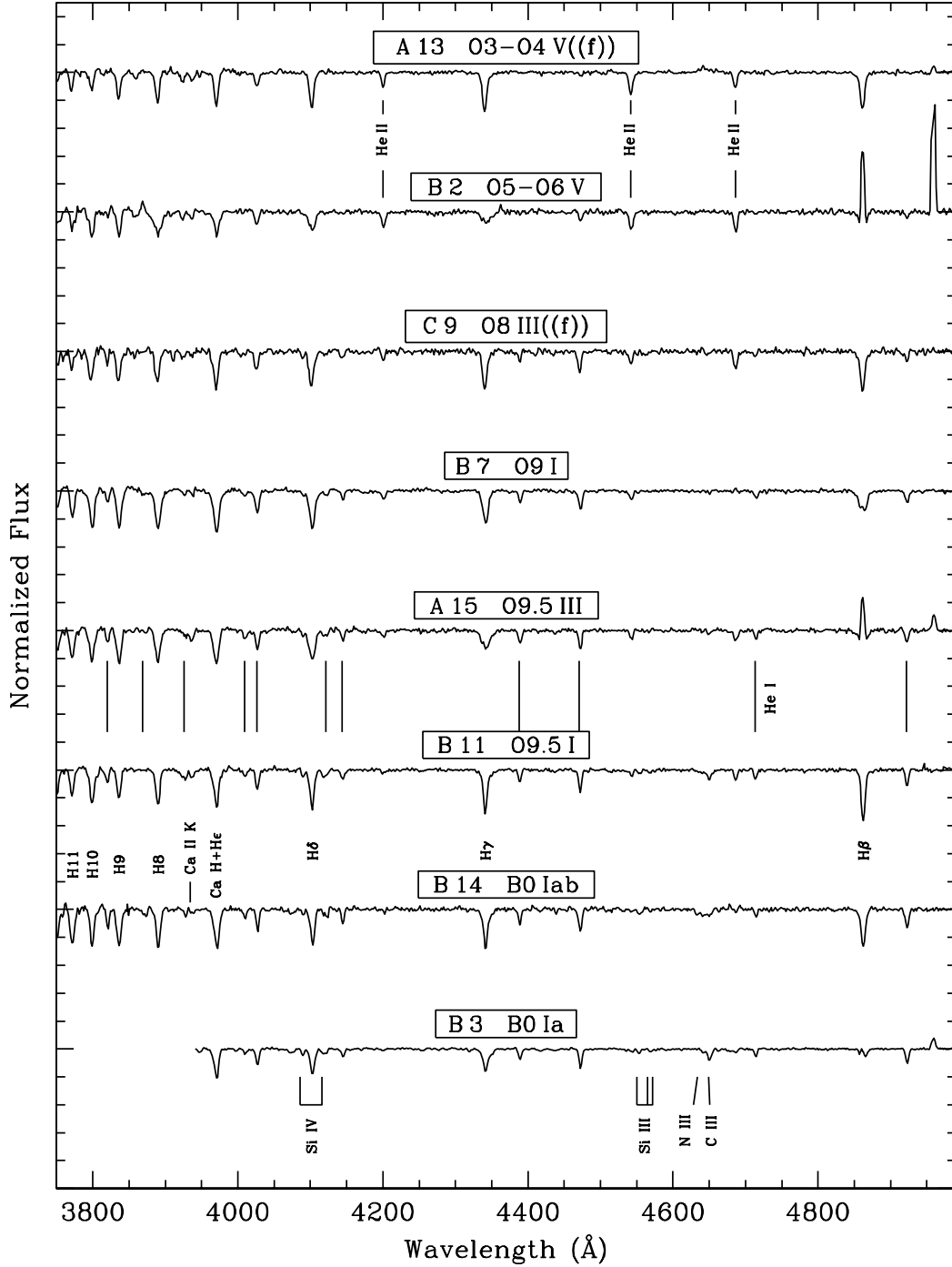


FIG. 3.— Normalized spectra of the O and B0 stars. The spectral features identified are He II  $\lambda\lambda$ 4200, 4542, 4686 (*below A13*); He I  $\lambda\lambda$ 3820, 3867-3872, 3926, 4009, 4026, 4121, 4144, 4388, 4471, 4713, 4922 (*below A15*); Balmer lines from H $\beta$  to H11, and the Ca II K ( $\lambda$ 3933) and H ( $\lambda$ 3968) lines (*below B11*); Si IV  $\lambda\lambda$ 4089, 4116, Si III  $\lambda\lambda$ 4553, 4568, 4575, N III  $\lambda\lambda$ 4634, 4640-4642, C III  $\lambda$ 4650 (*below B3*). Here, and through Fig. 9, ordinate tick marks are drawn at intervals of 0.2 continuum flux units.

$\log Q(H^0) = 48.82$ . This corresponds to the ionizing flux output of an O6.5 V star (Martins et al. 2005).

**B3 (B0 Ia).**—The third brightest blue supergiant ( $M_V = -6.8$ ) is star B42 in the list by Sandage & Katem (1976). Our B0 classification derives from the presence of He II  $\lambda\lambda$ 4542, 4686 in its spectrum, with He II  $\lambda$ 4542 < Si III  $\lambda$ 4553 (the two lines are of equal strength at O9.7). The stellar spectrum is heavily contaminated by nebular lines (see, for example, the filled-in H $\beta$  line and [O III]  $\lambda$ 5007 in emission). Humphreys (1980) obtained a spectrum of this star, and assigned a B0 classification based on two-color photometry. This is the only

star we have in common with Lozinskaya et al. (2002), who classified it (their star I.1) as an O supergiant.

**B17 (WO3).**—The Wolf-Rayet features in the bright star embedded in the H II region S3 were studied for the first time by D’Odorico & Rosa (1982, hence the name DR1) and Davidson & Kinman (1982). Spectra of this star have been discussed, among others, by Armandroff & Massey (1991), who classified it as WC4-5, Garnett et al. (1991, WO4) and Kingsburgh & Barlow (1995, WO3), whose classification we adopt. The spectrum (Fig. 10) is characterized by high-excitation nebular lines (including He II  $\lambda\lambda$ 4542, 4686, 5412)

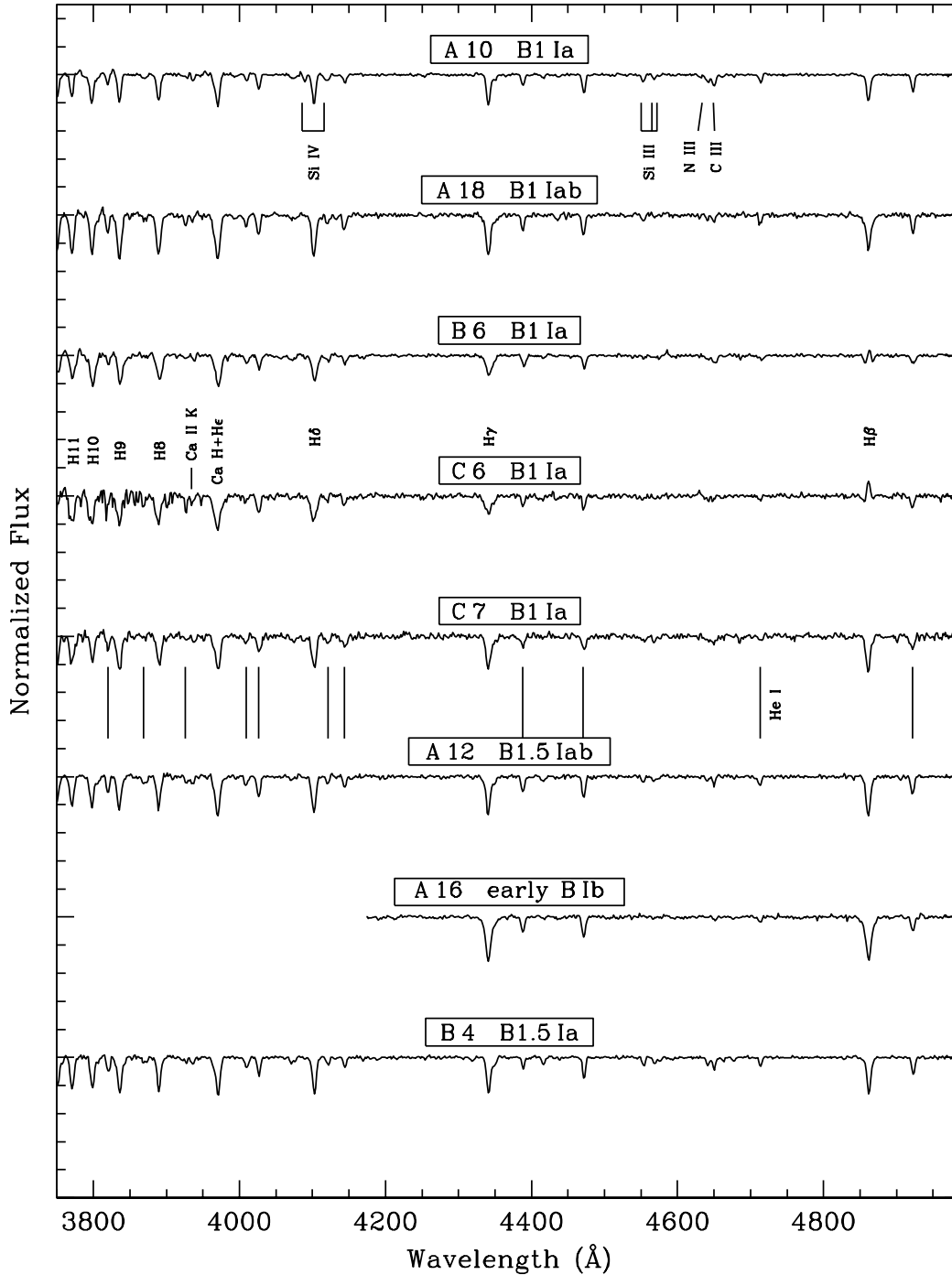


FIG. 4.— Normalized spectra of early-B stars (B1–B1.5). The spectral features identified are Si IV  $\lambda\lambda$ 4089, 4116, Si III  $\lambda\lambda$ 4553, 4568, 4575, N III  $\lambda\lambda$ 4634, 4640–4642, C III  $\lambda$ 4650 (*below A10*); Balmer lines from H $\beta$  to H11, and the Ca II K ( $\lambda$ 3933) and H ( $\lambda$ 3968) lines (*below B6*); He I  $\lambda\lambda$ 3820, 3867–3872, 3926, 4009, 4026, 4121, 4144, 4388, 4471, 4713, 4922 (*below C7*).

superposed on broad stellar lines from C IV, O V and O VI.

C5 (A V).—This star has a highly discrepant radial velocity,  $V_{\text{Helio}} = +17 \text{ km s}^{-1}$ , and its spectrum is characterized by narrow Balmer lines and very weak metal lines, with the exception of Ca II K. A halo dwarf A-type star or a lower-gravity, evolutionarily more evolved field horizontal branch star would both match these properties. Disentangling these two possibilities from linewidth measurements, even at higher resolution, is unfeasible for the coolest ( $B - V > 0.2$ ) A stars<sup>3</sup>

<sup>3</sup> We follow the terminology of Wilhelm et al. (1999b) and other works dealing with halo stars by including in the A-type class stars as cool as

(Arnold & Gilmore 1992). However, *UBV* photometry can be used to constrain  $T_{\text{eff}}$  and surface gravity, and we note that in the  $(U - B)_0$  vs.  $(B - V)_0$  color-color diagram shown by Wilhelm et al. (1999b) in their extensive study of A-type stars in the halo star C5 would fall in the A V domain. We adopted  $U - B = -0.18$  and  $B - V = 0.37$  (A. Herrero, private communication), and a Galactic reddening towards IC 1613  $E(B - V) = 0.025$  (Schlegel et al. 1998). We have used the model grid by Wilhelm et al. (1999a) to obtain approximate values of the stellar parameters from the *UBV* colors and the

$T_{\text{eff}} = 6000$ , i.e. what would be traditionally called F-type stars.

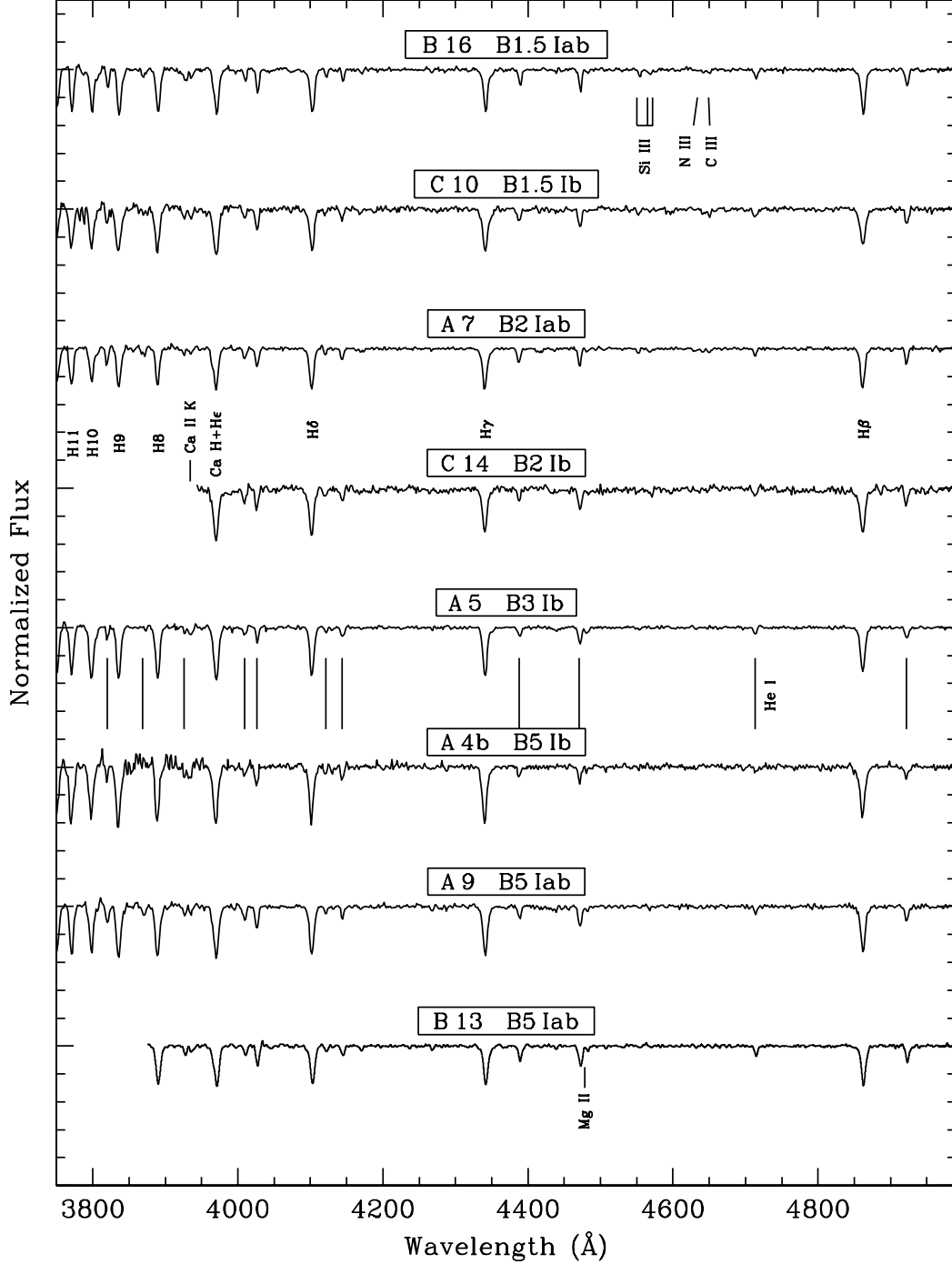


FIG. 5.— Normalized spectra of early- to mid-B stars (B1.5–B5). The spectral features identified are Si III  $\lambda\lambda$ 4553, 4568, 4575, N III  $\lambda\lambda$ 4634, 4640–4642, C III  $\lambda$ 4650 (*below B16*); Balmer lines from H $\beta$  to H11, and the Ca II K ( $\lambda$ 3933) and H ( $\lambda$ 3968) lines (*below A7*); He I  $\lambda\lambda$ 3820, 3867–3872, 3926, 4009, 4026, 4121, 4144, 4388, 4471, 4713, 4922 (*below A5*) and Mg II  $\lambda$ 4481 (*below B13*).

equivalent width of the Ca II K line. Our results,  $T_{\text{eff}} = 6750$  K,  $\log g = 4.0$ , and  $[\text{Fe}/\text{H}] = -2.0$ , confirm that C5 is a dwarf star. From an absolute magnitude  $M_V = 3.6$ , corresponding to the star's  $(B - V)_0$  color (Schmidt-Kaler 1982), we derive a distance of 8.1 kpc. We note that the Ca II K/(Ca II H + He) criterion provides an A5 classification.

*Be stars*—The group of 6 stars in Fig. 9 displays similar characteristics, with Balmer lines, as well as several Fe II lines, in emission. While H $\alpha$  and H $\beta$  are in emission for all stars, H $\gamma$  progresses from a filled-in profile to an emission line as  $\text{EW}(\text{H}\alpha)$  increases. The strength of the Fe II emission appears to be correlated with that of the H lines. The He I  $\lambda$ 5876

is seen in emission in all stars. The simultaneous presence of H, He and iron emission lines in B stars is consistent with the Group I Be classification of Jaschek et al. (1980). The definition of the B sub-class is made highly uncertain by the broadening of the lines (due to high rotational velocities) and the superposition of the Fe II  $\lambda\lambda$ 4549–4556, 4583 emission lines, originating in the surrounding shells, on top of the photospheric Si II  $\lambda\lambda$ 4553, 4568, 4575 lines. However, Be stars belonging to Group I are mostly of early-B type (B0–B3), and we detect a broad feature corresponding to the CNO blend at  $\sim 4650$  Å, found in early-B stars. We also detect He II  $\lambda$ 4686 in a few cases (e.g. A19, A17), pointing to an earlier, Oe star

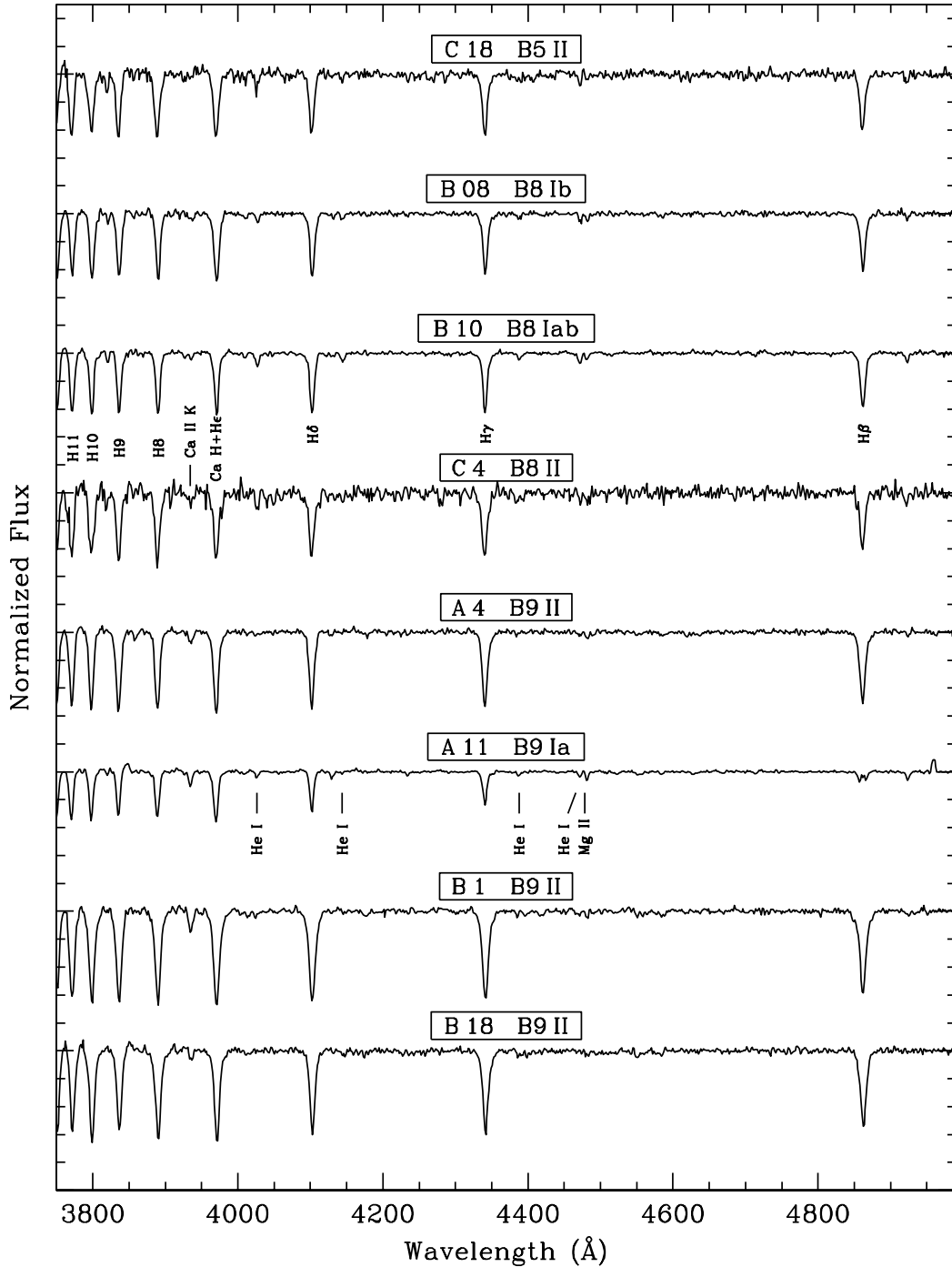


FIG. 6.— Normalized spectra of mid- to late-B stars (B5–B9). The spectral features identified are Balmer lines from  $H\beta$  to  $H11$ , and the  $\text{Ca II K}$  ( $\lambda 3933$ ) and  $\text{H}$  ( $\lambda 3968$ ) lines (*below B10*);  $\text{He I } \lambda\lambda 4026, 4121, 4388, 4471$  and  $\text{Mg II } \lambda 4481$  (*below A11*).

classification (Conti & Leep 1974). Absolute visual magnitudes range between  $M_V = -5.6$  (B12) and  $M_V = -4.4$  (A19). These values are comparable to those found for the brightest Be stars in the SMC (Martayan et al. 2007). The large number of Be stars found in our study tends to confirm the trend of increasing frequency of Be stars with decreasing metallicity (Maeder et al. 1999; Wisniewski & Bjorkman 2006).

*G stars*—Both C12 (type G2) and C15 (type G8, not shown in the spectral catalog) have a radial velocity which is discrepant with respect to the systemic velocity of IC 1613, as well as a bright apparent magnitude ( $V = 16.39$  and  $15.69$ , respectively), indicating that they are foreground Milky Way

stars. The classification is based on the strength of the G-band and  $\text{Fe I } \lambda 4325$  relative to  $\text{H}\gamma$  (Evans et al. 2004). The photometric parameters for these stars violate the criteria we use to select blue supergiants in external galaxies. These objects were included in the spectroscopic sample in order to fill otherwise unused slitlets of our MOS setup.

#### 4. STELLAR ABUNDANCES: B SUPERGIANTS

For the 9 early-B supergiants with the highest signal-to-noise ratio we have derived stellar parameters and metal abundances by comparing our observations with model spectra obtained with the FASTWIND code (Santolaya-Rey et al. 1997, Puls et al. 2005). Our procedure has been explained in de-



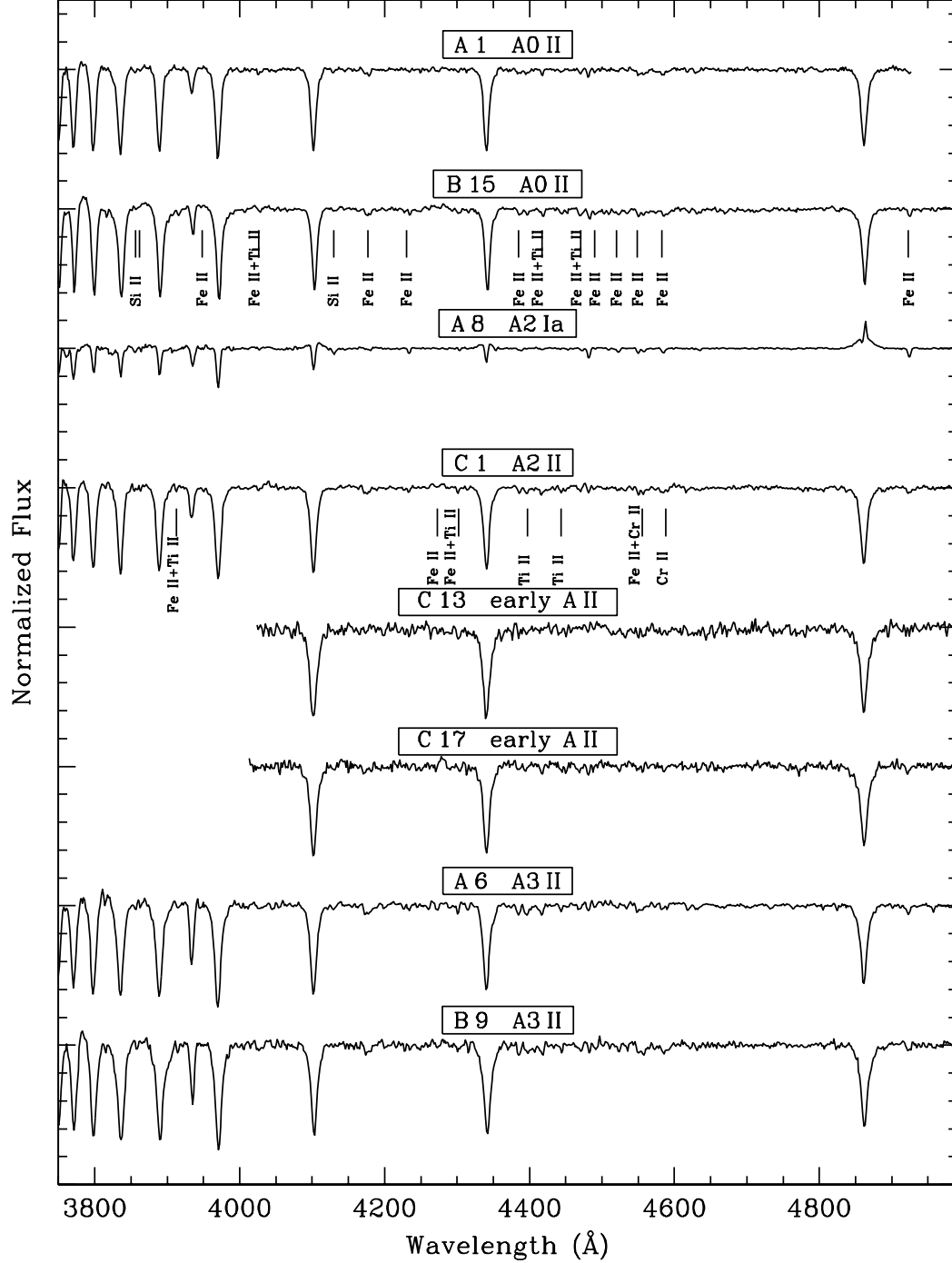


FIG. 7.— Normalized spectra of early-A stars (A0–A3). The spectral features identified are Si II  $\lambda\lambda$ 3856–3862, 4128–4132, Fe II  $\lambda\lambda$ 3945, 4024, 4173–4178, 4233, 4385, 4417, 4473, 4489–4491, 4549, 4583, 4923, and Ti II  $\lambda\lambda$ 4028, 4418, 4469–4471 (*below B15*); Fe II  $\lambda\lambda$ 3914, 4273, 4303, 4556, Ti II  $\lambda\lambda$ 3913, 4300, 4395–4399, 4444, and Cr II  $\lambda\lambda$ 4588, 4559 (*below C1*).

tail by Urbaneja et al. (2003, 2005), and has been recently used for the analysis of B supergiants in WLM (Bresolin et al. 2006) and NGC 3109 (Evans et al. 2007). As already mentioned in these papers, our best-fit models are those that provide the overall best match to the ensemble of metal lines present in the spectra, while some of the individual lines might be still not well reproduced. At the low abundances encountered in the dwarf irregular galaxies that we have so far analyzed [ $12 + \log(\text{O}/\text{H}) < 8.0$ ], the low spectral resolution and the limited signal-to-noise ratio that are available to us conspire to increase the uncertainty in the metallicity measurements, which for a single chemical element in a given star is

on the order of 0.2–0.25 dex. However, combining the information obtained from several stars, we can still obtain a meaningful picture of the content of the most abundant elements, in particular oxygen, in galaxies at relatively large distances, and verify, within the above-mentioned limits of precision, the presence of chemical inhomogeneities and the agreement with chemical abundances obtained with alternative means, in particular from the emission lines of H II regions (Bresolin et al. 2006).

The modeling with FASTWIND provides us with effective temperatures ( $T_{\text{eff}}$ ) from the helium (late-O stars) and silicon (early-B stars) ionization equilibria, while fits to the

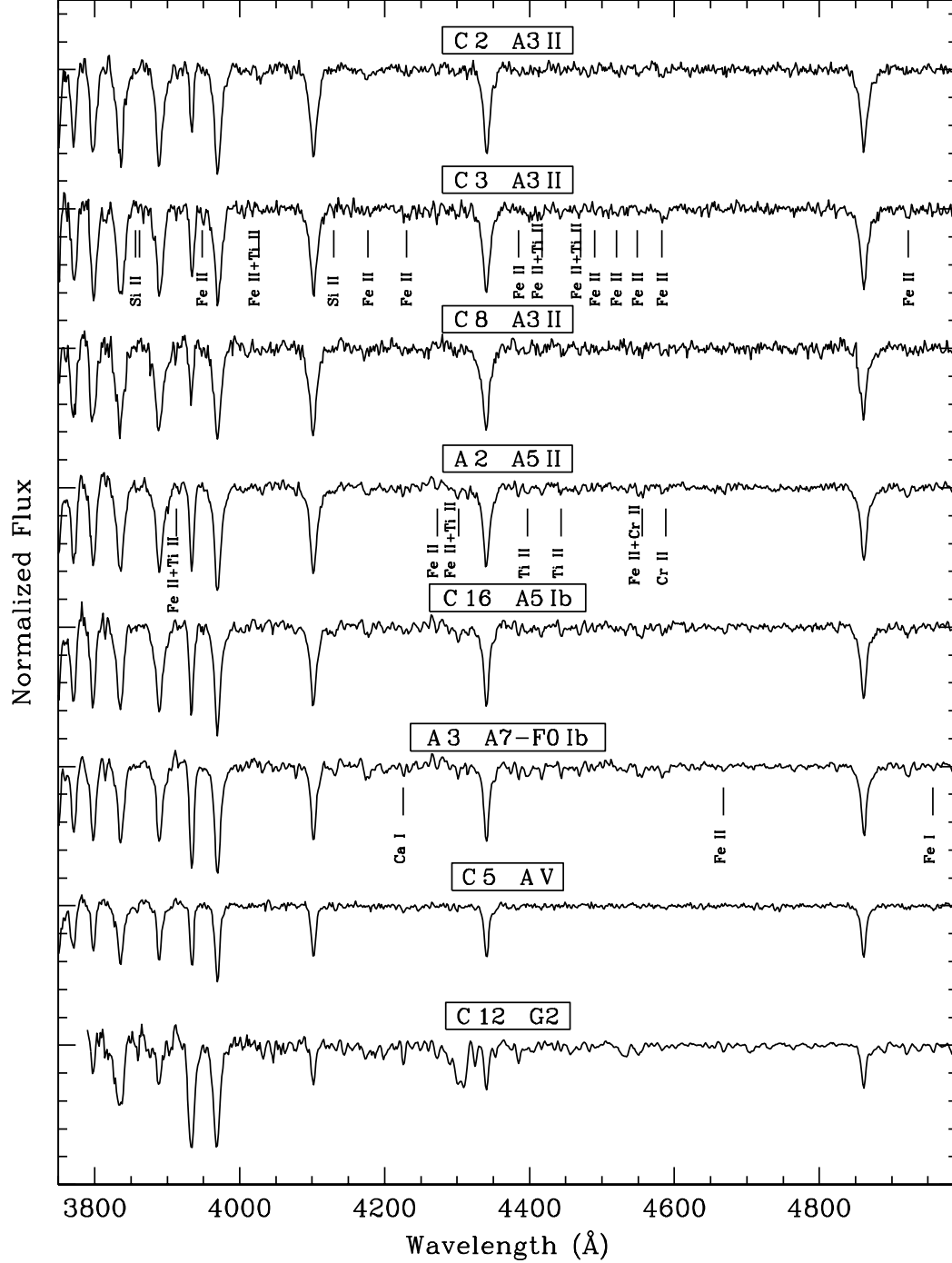


FIG. 8.— Normalized spectra of mid-A to G stars (A3–G2). The last two stars shown, C5 and C12, are foreground Galactic objects. The spectral features identified are Si II  $\lambda\lambda$ 3856–3862, 4128–4132, Fe II  $\lambda\lambda$ 3945, 4024, 4173–4178, 4233, 4385, 4417, 4473, 4489–4491, 4549, 4583, 4923, and Ti II  $\lambda\lambda$ 4028, 4418, 4469–4471 (*below* C3); Fe II  $\lambda\lambda$ 3914, 4273, 4303, 4556, Ti II  $\lambda\lambda$ 3913, 4300, 4395–4399, 4444, and Cr II  $\lambda\lambda$ 4588, 4559 (*below* A2); Fe II  $\lambda\lambda$ 4666–4669, Fe I  $\lambda$ 4957, and Ca I  $\lambda$ 4226 (*below* A3).

Balmer line profiles are used to determine surface gravities ( $\log g$ ). Among the additional parameters that are estimated by the fitting procedure are the microturbulent velocity,  $v_{\text{turb}}$  (using a combination of He I and the Si II/III/IV lines) and the abundances of various metals. The main abundance diagnostics used in this work are C II  $\lambda\lambda$ 6578–6583; N II  $\lambda\lambda$ 3995, 5050, 5100; O II  $\lambda\lambda$ 4072–4076, 4317–4319, 4414–4416; Mg II  $\lambda$ 4481; Si III  $\lambda\lambda$ 4553–4575. One or more of these features are not always available with sufficient S/N to provide strong constraints on the chemical abundance. However, the large number of additional faint metal lines and

line blends that are present in the optical range, especially originated by oxygen atoms, is used to determine the metal content even when individual lines cannot be resolved in our spectra. For the He abundance we rely on He I  $\lambda\lambda$ 4026, 4388, 4471, 4921, 5015, 5048 and 6678 (the other lines have uncertain broadening data). The reddening for each star has been derived from a comparison of the observed *VI* and *JK* magnitudes (the latter extracted from the near-IR photometry by Pietrzyński et al. 2006) with the spectral energy distribution of the best-fitting FASTWIND models, and adopting the Cardelli et al. (1989) extinction law with  $R_V = 3.1$ . We ob-

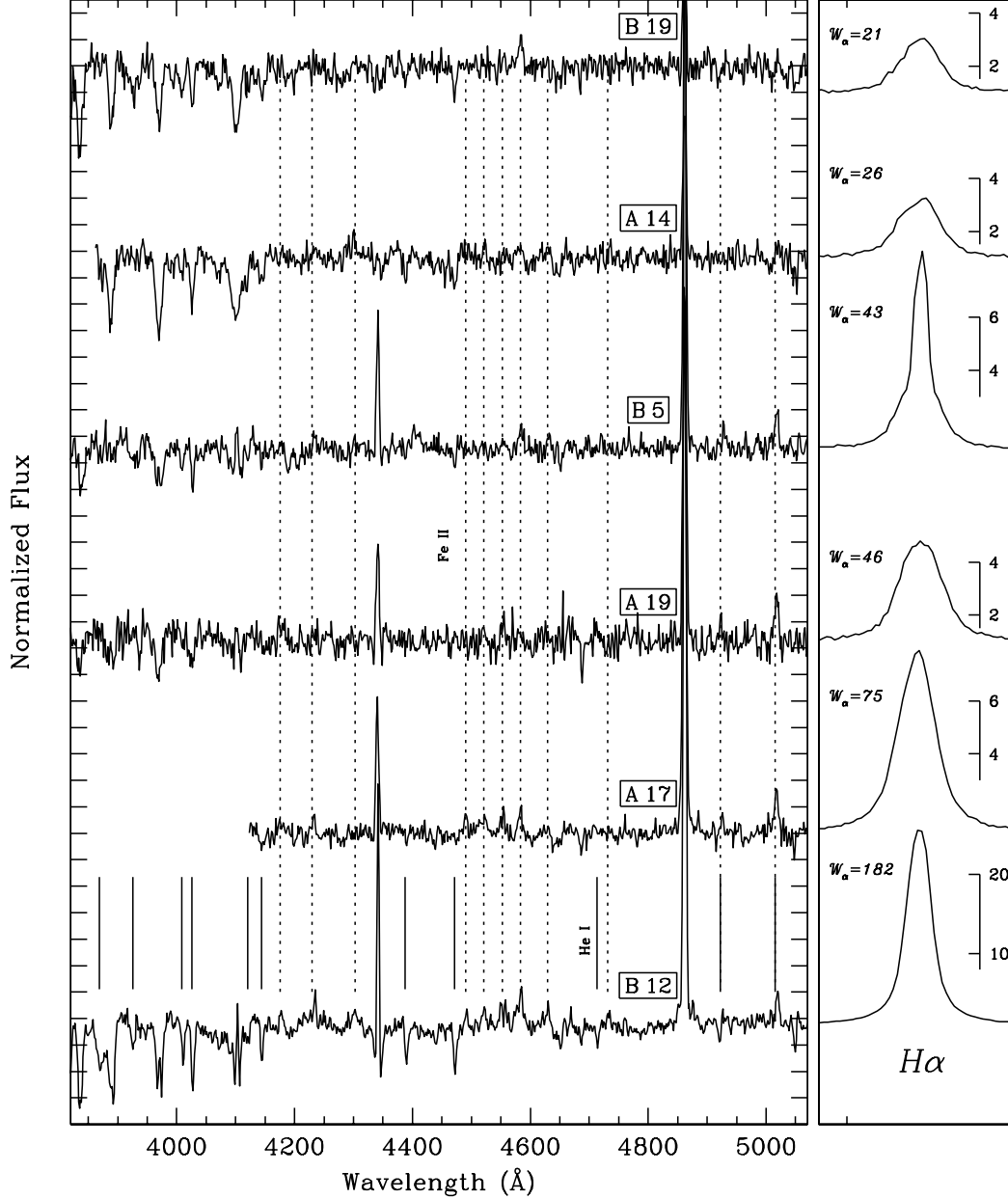


FIG. 9.— Normalized spectra of the Be stars, in order of increasing strength of the  $H\alpha$  emission (the  $H\beta$  line is clipped for clarity). The dotted lines mark the wavelengths of the Fe II lines  $\lambda\lambda 4173\text{--}4178, 4233, 4303, 4489\text{--}4491, 4520\text{--}4523, 4549\text{--}4556, 4583, 4629, 4731, 4922, 5015$ . The wavelengths of the following neutral helium lines are indicated at the bottom: He I  $\lambda\lambda 3867\text{--}3872, 3926, 4009, 4026, 4121, 4144, 4388, 4471, 4713, 4922, 5015$ . The panel on the right displays the profile of the  $H\alpha$  line, using different vertical stretches. The equivalent width of the line,  $W_\alpha$ , is indicated to the left of each profile. The spectrum of star B5 is affected by nebular emission.

tain rather low values for  $E(B - V)$ , with a mean value of  $0.06 \pm 0.03$ , similar to the result of  $0.09 \pm 0.02$  obtained independently in our Cepheid study (Pietrzyński et al. 2006).

Our results are summarized in Table 3, where the chemical abundances of C, N, O, Mg and Si are expressed with the notation  $\epsilon_X = 12 + \log(X/H)$ . The distance-dependent parameters assume a distance to IC 1613 of 721 kpc (Pietrzyński et al. 2006). Our estimated errors are 1000 K in  $T_{\text{eff}}$ , 0.1 dex in  $\log g$ , and vary between 0.17 dex and 0.25 dex in metal abundances. Spectroscopic masses  $M_{\text{spec}}$  are lower limits, due to the fact that at the FORS spectral resolution we cannot determine corrections to the gravities that account for the stellar rotational velocities. The sensitivity of the derived chemical abundances to the different stellar parameters for stars of similar  $T_{\text{eff}}$  and from similar data as ours have been presented in detail by

Urbaneja et al. (2005) and Evans et al. (2007), and will not be repeated here. In Fig. 11 and 12 we plot the adopted final models on top of the observed spectra for the 9 B-type supergiants we have analyzed. Fig. 13 presents a comparison between the spectrum of the B2 Iab star A7 in the 4300–4700 Å wavelength range and FASTWIND models calculated at the adopted metallicity (for oxygen:  $\epsilon_O = 7.85 \pm 0.25$ , dotted line in the center), and at 0.2 dex higher (top) and lower (bottom) metal abundances. This example is a typical case: while overall the strength of the observed spectral features agree with the adopted model, some features (e.g. [O II]  $\lambda\lambda 4415\text{--}4417$  for this star) are better reproduced with the 0.2 dex higher abundance, while others (e.g. [O II]  $\lambda\lambda 4317\text{--}4319$  in this example) would suggest a slightly lower abundance.

The mean oxygen abundance of the stars in Table 3

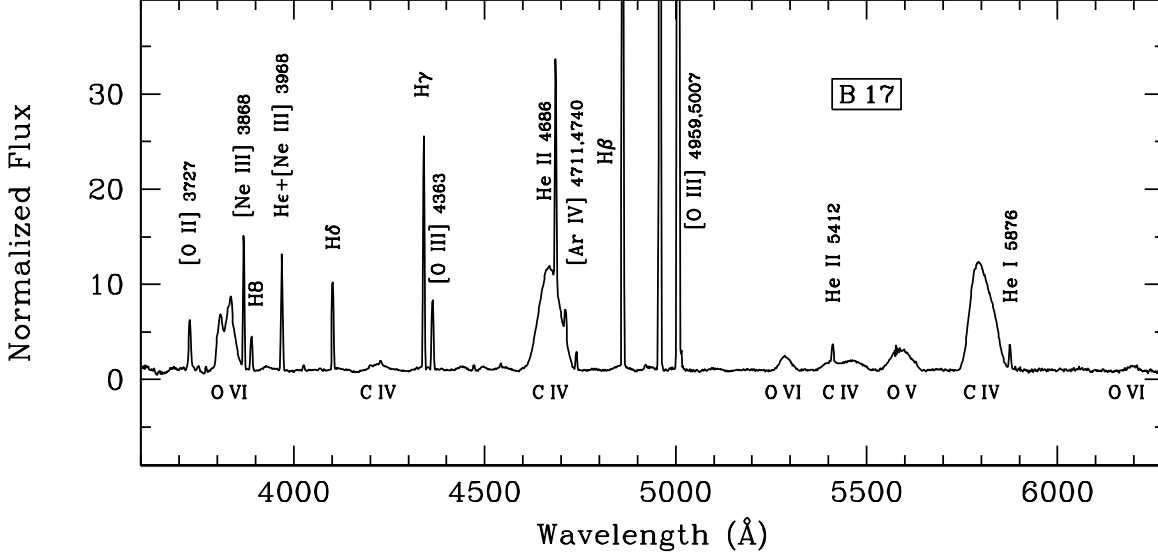


FIG. 10.— Normalized spectrum of the WO3 star B17. Broad stellar lines are identified at the bottom: O V  $\lambda$ 5590, O VI  $\lambda\lambda$ 3811-3834, 5290, 6200 and C IV  $\lambda\lambda$ 4229, 4658-4686, 5411-5470, 5801-5812. A number of nebular emission lines are also marked in the top portion of the figure.

TABLE 3  
PHYSICAL PARAMETERS OF B SUPERGIANTS

Properties	A7	A10	A12	A18	B3	B4	B11	B13	B16
Spectral type ...	B2 Iab	B1 Ia	B1.5 Iab	B1 Iab	B0 Ia	B1.5 Ia	O9.5 Iab	B5 Iab	B1.5 Iab
$T_{\text{eff}}$ (K) <sup>a</sup> .....	19500	25000	23000	21000	24500	22500	30000	17000	21000
$\log g$ (cgs) <sup>b</sup> .....	2.55	2.70	2.75	2.70	2.65	2.60	3.20	2.30	2.75
$R/R_{\odot}$ .....	$30 \pm 3$	$38 \pm 3$	$24 \pm 2$	$19 \pm 2$	$32 \pm 3$	$27 \pm 2$	$19 \pm 1$	$31 \pm 3$	$25 \pm 3$
B.C. ....	-1.89	-2.47	-2.32	-2.08	-2.42	-2.19	-2.19	-1.57	-2.09
$M_{\text{bol}}$ .....	-7.93	-9.55	-8.13	-7.14	-9.10	-8.26	-8.80	-7.40	-7.86
$\log L/L_{\odot}$ .....	$5.07 \pm 0.18$	$5.71 \pm 0.14$	$5.15 \pm 0.16$	$4.75 \pm 0.18$	$5.53 \pm 0.14$	$5.20 \pm 0.15$	$5.42 \pm 0.11$	$4.86 \pm 0.20$	$5.04 \pm 0.16$
$M_{\text{spec}}/M_{\odot}$ .....	$12 \pm 5$	$27 \pm 10$	$11 \pm 5$	$7 \pm 3$	$19 \pm 7$	$11 \pm 4$	$21 \pm 7$	$7 \pm 3$	$13 \pm 6$
$E(B-V)$ .....	0.04	0.08	0.11	0.00	0.06	0.04	0.09	0.03	0.10
$v_{\text{turb}}$ (km s <sup>-1</sup> ) ...	10	15	12	15	12	15	15	10	15
$Y_{\text{He}}$ .....	0.08	0.08	0.10	0.08	0.08	0.10	0.08	0.10	0.08
$\epsilon_{\text{C}}$ .....	$7.15 \pm 0.20$	$< 7.30$	$< 6.90$	$7.20 \pm 0.20$	...	$6.95 \pm 0.20$	$7.20 \pm 0.20$	...	$7.00 \pm 0.20$
$\epsilon_{\text{N}}$ .....	$7.40 \pm 0.25$	$7.10 \pm 0.20$	$7.10 \pm 0.20$	$< 7.65$	$< 7.20$	$7.00 \pm 0.20$	$7.10 \pm 0.20$	...	$7.30 \pm 0.20$
$\epsilon_{\text{O}}$ .....	$7.85 \pm 0.25$	$7.85 \pm 0.17$	$7.85 \pm 0.17$	$7.90 \pm 0.20$	$7.95 \pm 0.20$	$8.00 \pm 0.20$	$8.00 \pm 0.20$	...	$7.80 \pm 0.20$
$\epsilon_{\text{Mg}}$ .....	$6.80 \pm 0.20$	$< 6.90$	$< 6.75$	$< 6.75$	...	$< 6.60$	...	$6.90 \pm 0.20$	$6.75 \pm 0.20$
$\epsilon_{\text{Si}}$ .....	$6.65 \pm 0.20$	$6.90 \pm 0.20$	$6.65 \pm 0.20$	$6.60 \pm 0.20$	$6.65 \pm 0.20$	$6.60 \pm 0.20$	$6.60 \pm 0.20$	$6.60 \pm 0.20$	$6.60 \pm 0.20$
[O/H] <sup>c</sup> (dex) ....	-0.85	-0.85	-0.85	-0.80	-0.75	-0.70	-0.70	...	-0.9

NOTE. — Abundances are expressed as  $\epsilon_X = 12 + \log(X/H)$ .

<sup>a</sup> Error:  $\pm 1000$  K. <sup>b</sup> Error:  $\pm 0.10$ . <sup>c</sup> Adopting  $\epsilon_{\text{O},\odot} = 8.66$  (Asplund et al. 2004).

is  $12 + \log(\text{O}/\text{H}) = 7.90 \pm 0.08$ . In Section 5 we obtain from two H II regions an average nebular abundance  $12 + \log(\text{O}/\text{H}) = 7.73 \pm 0.03$ . In view of the errors, we regard the slight discrepancy as not significant. The median oxygen abundance of the B supergiants of 7.9 compares to very similar values of 7.9 obtained in WLM (Bresolin et al. 2006) and of 7.8 in NGC 3109 (Evans et al. 2007).

Regarding the additional chemical elements, in several cases we could only obtain upper limits to their abundances, except for silicon. Nitrogen abundances could be measured for 6 stars. They are considerably higher than the H II region values of  $12 + \log(\text{N}/\text{H}) = 6.5\text{--}6.7$  (Lee et al. 2003, Kingsburgh & Barlow 1995), by up to  $\sim 0.7$  dex. Nitrogen enrichments of comparable size are found in samples of B supergiants in, for example, the SMC (Trundle et al. 2004). Excluding upper limits, the mean abundances (by number of particles) of the remaining elements relative to oxygen,  $\log(\text{C}/\text{O}) = -0.8$ ,  $\log(\text{Si}/\text{O}) = -1.20$  and

$\log(\text{Mg}/\text{O}) = -1.05$ , are also comparable to the SMC B supergiant values (Dufton et al. 2005).

## 5. NEBULAR ABUNDANCES

Several of our stellar spectra show contamination by nebular lines, as summarized in the last column of Table 1. This offers us the possibility of comparing H II region chemical abundances with the metallicities derived for the supergiant stars. In order to determine accurate nebular abundances, the knowledge of the electron temperature of the gas,  $T_e$ , is necessary, since the emissivities of the forbidden lines used for nebular abundance work strongly depend on it. At low metallicity the auroral-to-nebular line ratio  $[\text{O III}] \lambda 4363 / (\lambda 4959 + \lambda 5007)$  can be used for such purpose. However, the H II regions in IC 1613 are of low surface brightness, making it difficult to detect the faint  $\lambda 4363$  auroral line. Abundance measurements based on this line have been carried out in the H II region S3 (Sandage 1971) by several authors, thanks to the high degree of excitation of this nebula, ionized by the hot WO3 star de-

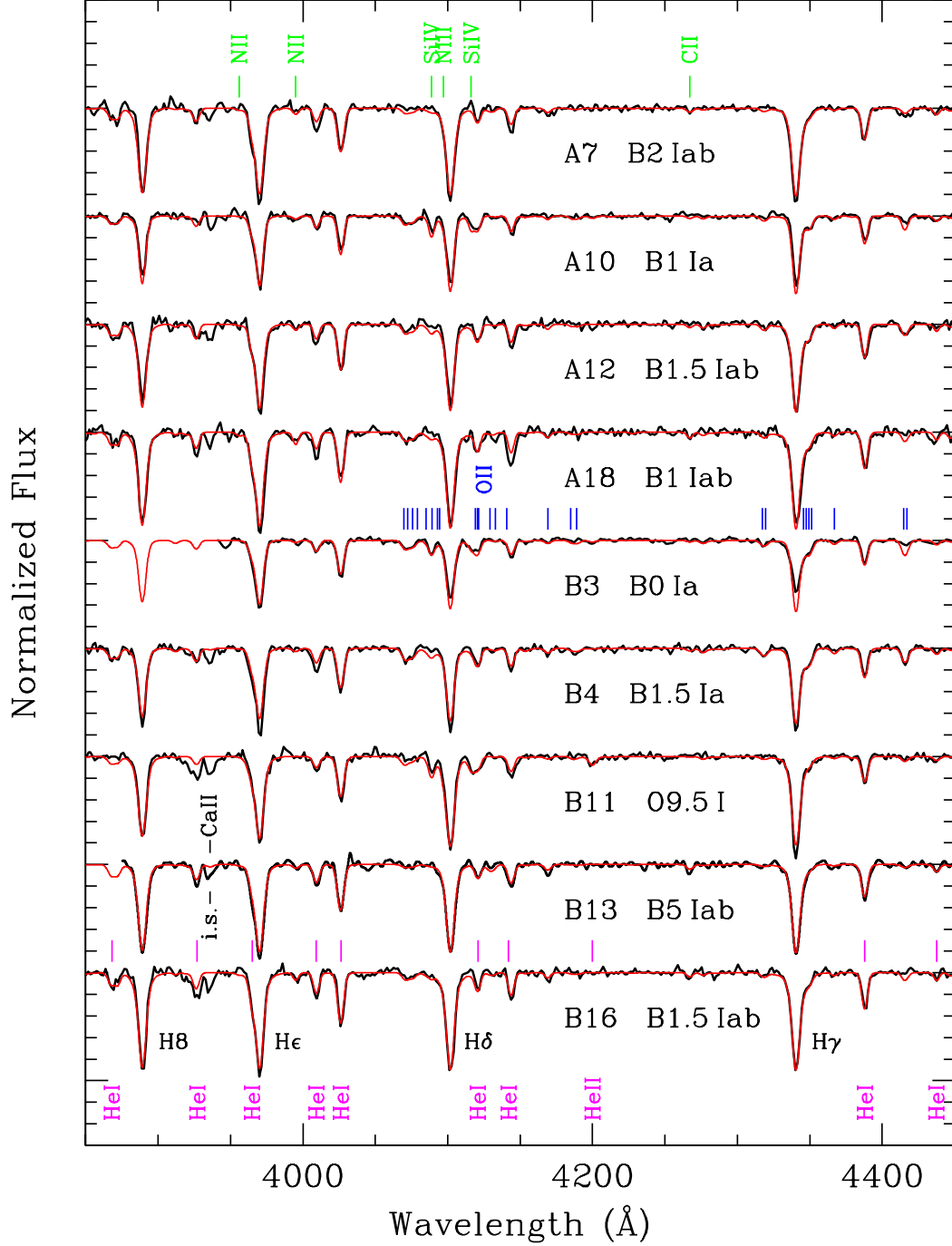


FIG. 11.— Comparison between the observed spectra (thick dark lines) and the adopted FASTWIND models (red lines) in the 3850–4450 Å range. Identifications for the H, He and some of the metal lines are provided. Here, and in Fig. 12, ordinate tick marks are drawn at intervals of 0.2 continuum flux units.

scribed previously, that makes the [O III] lines very strong. In their early work Davidson & Kinman (1982) obtained an oxygen abundance  $12 + \log(\text{O}/\text{H}) = 7.87$ , while more modern measurements by Kingsburgh & Barlow (1995) and Lee et al. (2003) are in the range  $12 + \log(\text{O}/\text{H}) = 7.62\text{--}7.70$ . Work on additional H II regions has derived chemical abundances from bright-line methods and comparisons of the line flux ratios to photoionization model results, without a direct measurement of the electron temperature. In particular, the chemical abundance for the supernova remnant S8 has been studied by D’Odorico & Dopita (1983,  $12 + \log(\text{O}/\text{H}) = 7.60$ ) and Peimbert et al. (1988,  $12 + \log(\text{O}/\text{H}) = 7.83$ ). Lee et al. (2003) determined  $12 + \log(\text{O}/\text{H}) = 7.90$  for region #13 (Hodge et al.

1990) from the  $R_{23}$  method. A N/O ratio enhanced relative to other low-luminosity dwarf irregular galaxies, in the range  $\text{N}/\text{O} = 0.07\text{--}0.12$ , is found in the papers cited.

Two stars in our sample are associated with H II regions in which we have detected [O III]  $\lambda 4363$ : B17 (H II region S3) and B2 (H II region S17). For the spectral extraction of these two H II regions we have avoided the stars, thus producing nebular spectra that are unaffected by strong stellar continua (Fig. 14). As already known since the early studies of the WO3 star DR1 and its associated nebula (D’Odorico & Rosa 1982; Davidson & Kinman 1982), the high-excitation spectrum of S3 contains the rare He II  $\lambda 4686$  line. In our spectrum we have also detected the fainter He II  $\lambda 4542$  and  $\lambda 5412$

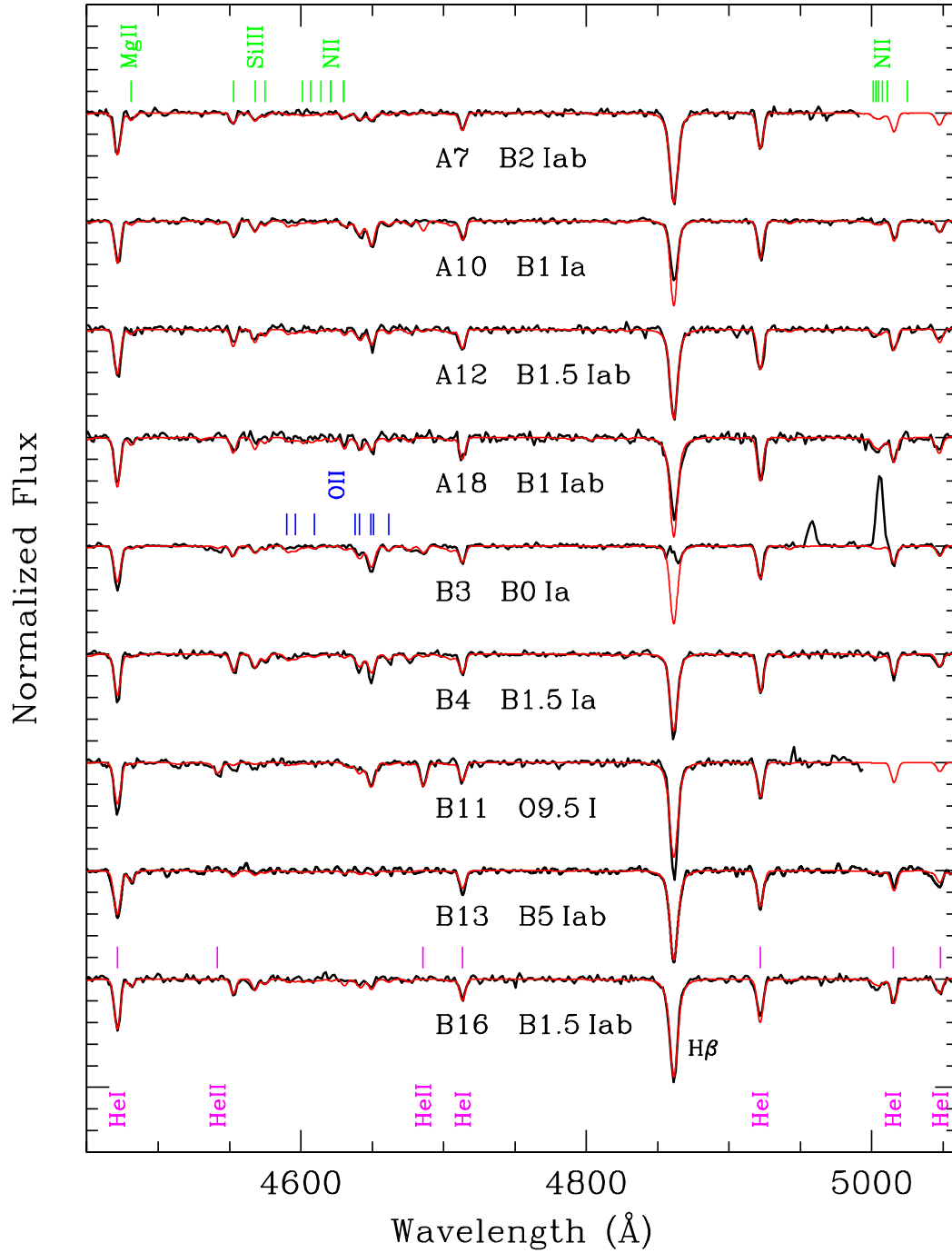


FIG. 12.— Same as Fig. 11, for the 4450–5065 Å range.

lines.

The emission line intensities, measured after flux-calibration of the spectra, and normalized to  $I(\text{H}\beta) = 100$ , are presented in Table 4. The Balmer decrement, measured by the  $\text{H}\gamma/\text{H}\beta$  and  $\text{H}\delta/\text{H}\beta$  line ratios, is consistent with a negligible amount of extinction for both H II regions. We have derived the electron temperature for the  $\text{O}^{++}$ -emitting zone,  $T(\text{O III})$ , from the  $[\text{O III}] \lambda 4363 / (\lambda 4959 + \lambda 5007)$  ratio and assuming the low-density regime ( $N_e = 100 \text{ cm}^{-3}$ ), using the *nebular* package in IRAF. Our value for S3,  $T_e = 18300 \pm 400 \text{ K}$ , compares well with  $T_e = 17910 \text{ K}$  given by Lee et al. (2003), and is slightly higher than  $T_e = 17100 \pm 500 \text{ K}$  reported by Kingsburgh & Barlow (1995). The temperature of the  $\text{O}^{+}$ -

emitting zones,  $T(\text{O II})$ , has been derived from  $T(\text{O III})$  and the relations published by Izotov et al. (2006). The oxygen ionic abundances,  $\text{O}^{+}/\text{H}^{+}$  (obtained from  $[\text{O II}] \lambda 3727/\text{H}\beta$ ) and  $\text{O}^{++}/\text{H}^{+}$  (from  $[\text{O III}] \lambda 5007/\text{H}\beta$ ), together with additional parameters, are summarized in Table 5.

For the H II region S17 the total oxygen abundance is given as the sum  $\text{O}^{+}/\text{H}^{+} + \text{O}^{++}/\text{H}^{+}$ , and we obtain  $12 + \log(\text{O}/\text{H}) = 7.78 \pm 0.05$ . For the high excitation region S3 we need to account for the contribution of  $\text{O}^{3+}$ , which is not observed in the optical range. To estimate an ionization correction factor (ICF) we have followed Kingsburgh & Barlow (1994):  $\text{ICF}(\text{O}) = (1 + \text{He}^{++}/\text{He}^{+})^{2/3} = 1.24$ . With

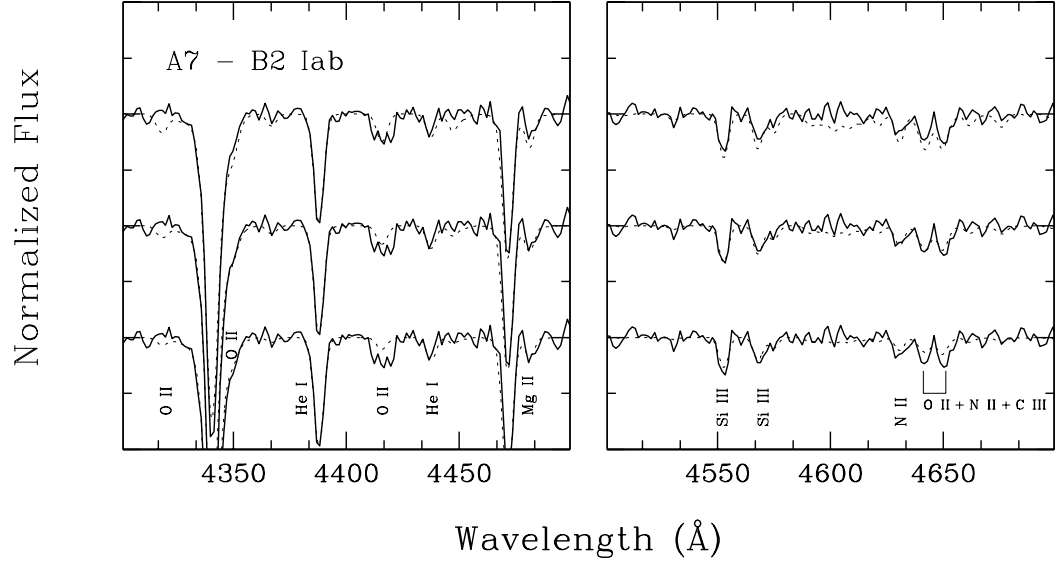


FIG. 13.— Comparison between the observed spectrum of the B2 Iab star A7 (solid lines) with FASTWIND models calculated by varying the metal abundances by  $\pm 0.2$  dex (dotted lines, top and bottom spectra, respectively) relative to the adopted metallicity (dotted line, central spectra). The spectral features identified are O II  $\lambda\lambda$  4317-4319, 4346-4351, 4415-4417; He I  $\lambda\lambda$  4388, 4438; Mg II  $\lambda$  4481; Si III  $\lambda\lambda$  4553, 4568, 4575; N II  $\lambda$  4630, and the O II + N II + C III blend at  $\lambda$  4650.

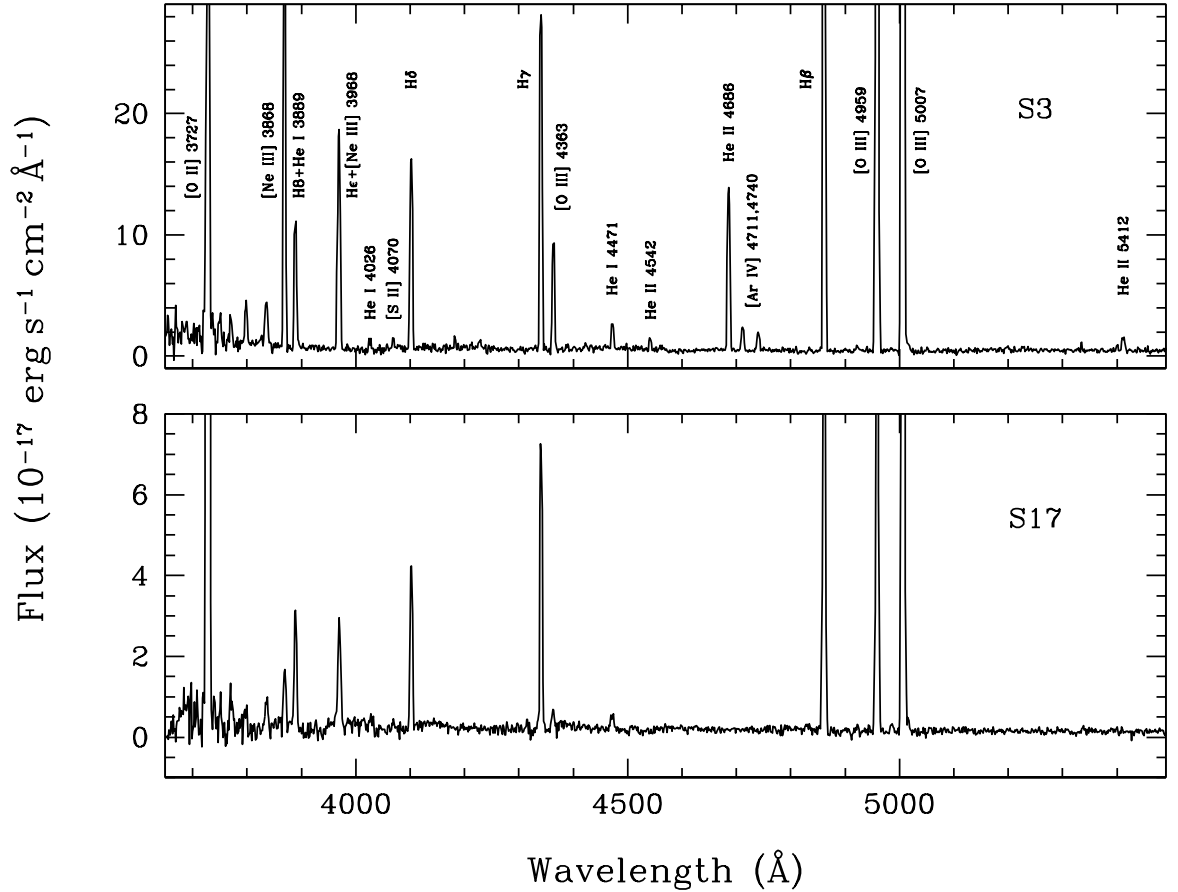


FIG. 14.— Spectra of the H II regions S3 (top) and S17 (bottom). The main nebular lines are identified.

TABLE 4  
H II REGIONS: REDDENING-CORRECTED LINE FLUXES

$\lambda_0$ (Å)	Ion	S3	S17
3727.....	[O II]	$93 \pm 5$	$299 \pm 15$
3869.....	[Ne III]	$55 \pm 3$	$10.9 \pm 0.9$
3889.....	H I + He I	$18.6 \pm 0.9$	$20.4 \pm 1.2$
3969.....	H I + [Ne III]	$34 \pm 2$	$22.7 \pm 1.4$
4026.....	He I	$1.8 \pm 0.3$	...
4072.....	[S II]	$1.2 \pm 0.4$	...
4101.....	H I	$27 \pm 1$	$26 \pm 1$
4340.....	H I	$50 \pm 2$	$49 \pm 2$
4363.....	[O III]	$15.1 \pm 0.6$	$3.9 \pm 0.4$
4471.....	He I	$3.6 \pm 0.2$	$3.2 \pm 0.4$
4686.....	He II	$24.1 \pm 0.9$	...
4711.....	[Ar IV]	$3.5 \pm 0.2$	...
4740.....	[Ar IV]	$2.7 \pm 0.2$	...
4861.....	H I	$100 \pm 4$	$100 \pm 4$
4922.....	He I	$1.04 \pm 0.32$	...
4959.....	[O III]	$183 \pm 7$	$73 \pm 3$
5007.....	[O III]	$521 \pm 20$	$221 \pm 9$
5412.....	He II	$2.4 \pm 0.2$	...
5876.....	He I	$7.1 \pm 0.4$	$11.4 \pm 0.7$

NOTE. — Fluxes are normalized to  $H\beta = 100$ .

TABLE 5  
H II REGIONS: DERIVED PARAMETERS

	S3	S17
$T(\text{O III})$ .....	$18300 \pm 400$	$14500 \pm 700$
$T(\text{O II})$ .....	$14900 \pm 50$	$13600 \pm 400$
$\text{O}^+/\text{H}^+$ .....	$(7.0 \pm 0.1) \times 10^{-6}$	$(3.4 \pm 0.3) \times 10^{-5}$
$\text{O}^{++}/\text{H}^+$ .....	$(3.5 \pm 0.2) \times 10^{-5}$	$(2.6 \pm 0.3) \times 10^{-5}$
$\text{He}^+/\text{H}^+$ .....	$0.057 \pm 0.004$	$0.092 \pm 0.007$
$\text{He}^{++}/\text{H}^+$ .....	$0.022 \pm 0.001$	...
$\text{ICF}(\text{O})$ .....	1.24	1
$12 + \log(\text{O}/\text{H})$ .....	$7.63 \pm 0.02$	$7.78 \pm 0.05$
$12 + \log(\text{O}/\text{H})_c^a$ .....	$7.72 \pm 0.02$	$7.78 \pm 0.05$
$\text{He}/\text{H}$ .....	$0.079 \pm 0.005$	$0.092 \pm 0.007$

<sup>a</sup> Oxygen abundance corrected for the ionization correction factor  $\text{ICF}(\text{O})$ .

this correction, the oxygen abundance of S3 becomes  $12 + \log(\text{O}/\text{H}) = 7.72 \pm 0.02$ . This value agrees with the result by Kingsburgh & Barlow (1995,  $12 + \log(\text{O}/\text{H}) = 7.70$ ). Lee et al. (2003) obtained  $12 + \log(\text{O}/\text{H}) = 7.62 \pm 0.05$ , but they did not apply any correction to account for the presence of  $\text{O}^{3+}$ . Our uncorrected value is  $12 + \log(\text{O}/\text{H}) = 7.63 \pm 0.02$ .

To summarize, besides the well-studied H II region S3, ionized by the WO3 star DR1, with this study we have found a second H II region in IC 1613 in which we have

a direct measurement of the electron temperature. The oxygen abundances of two H II regions agree quite well, with an average  $12 + \log(\text{O}/\text{H}) = 7.73 \pm 0.04$ . We also note the good agreement found between nebular and stellar helium abundances: the mean from the B supergiants is  $\text{He}/\text{H} = 0.087 \pm 0.010$ , while the weighted mean from the H II regions is  $\text{He}/\text{H} = 0.083 \pm 0.009$ ,

## 6. SUMMARY

In this paper we have presented multi-object spectroscopy of young, massive stars that we have obtained in the Local Group galaxy IC 1613. We have provided the spectral classification and a detailed spectral catalog for 54 OBA stars in this galaxy. The majority of the photometrically selected sample is composed of B- and A-type supergiants. The remaining stars include early O-type dwarfs and the only Wolf-Rayet star known in this galaxy. Among the early B stars we have uncovered 6 Be stars, which constitute the largest spectroscopically confirmed sample of this class of objects beyond the Magellanic Clouds. The radial velocities of all these stars is consistent with the systemic velocity. Only three stars have clearly discrepant velocities, and are identified as foreground objects belonging to the Milky Way. Of these, 2 G-type stars clearly violate the criterion used for the selection of blue supergiants. The third one, an A star in the Galactic halo, has very weak metal lines, and would have been flagged as peculiar even in the absence of a discrepant radial velocity information.

Using model atmospheres calculated with FASTWIND we have measured chemical abundances for 9 early-B supergiants, and have found a mean oxygen abundance of  $12 + \log(\text{O}/\text{H}) = 7.90 \pm 0.08$ . This value is comparable with the result we obtain for two H II regions in which we detect the temperature-sensitive [O III]  $\lambda 4363$  auroral line,  $12 + \log(\text{O}/\text{H}) = 7.73 \pm 0.04$ . The agreement extends to the helium abundance. The abundance patterns we find for the remaining chemical elements is similar to those measured in B supergiants in the slightly more metal-rich SMC. The stellar oxygen abundance is very close to the values we have found from similar data in the other dwarf galaxies whose blue supergiants have been studied so far as part of the Araucaria project, WLM and NGC 3109.

FB would like to thank the ESO-Paranal staff for their high standard of support throughout this project. We thank A. Herrero for providing us with the *UBV* photometry. GP and WG gratefully acknowledge financial support for this work from the Chilean Center for Astrophysics, under grant FONDAP 15010003.

## REFERENCES

- Armandroff, T. E. & Massey, P. 1991, *AJ*, 102, 927  
 Arnold, R. & Gilmore, G. 1992, *MNRAS*, 257, 225  
 Asplund, M., Grevesse, N., Sauval, A. J., Allende Prieto, C., & Kiselman, D. 2004, *A&A*, 417, 751  
 Azzopardi, M. 1987, *A&AS*, 69, 421  
 Azzopardi, M., Lequeux, J., & Maeder, A. 1988, *A&A*, 189, 34  
 Borissova, J., Kurtev, R., Georgiev, L., & Rosado, M. 2004, *A&A*, 413, 889  
 Bresolin, F., Gieren, W., Kudritzki, R.-P., Pietrzyński, G., & Przybilla, N. 2002, *ApJ*, 567, 277  
 Bresolin, F., Pietrzyński, G., Urbaneja, M. A., Gieren, W., Kudritzki, R.-P., & Venn, K. A. 2006, *ApJ*, 648, 1007  
 Cardelli, J. A., Clayton, G. C., & Mathis, J. S. 1989, *ApJ*, 345, 245  
 Cole, A. A., Tolstoy, E., Gallagher, III, J. S., Hoessel, J. G., Mould, J. R., Holtzman, J. A., Saha, A., Ballester, G. E., Burrows, C. J., Clarke, J. T., Crisp, D., Griffiths, R. E., Grillmair, C. J., Hester, J. J., Krist, J. E., Meadows, V., Scowen, P. A., Stapelfeldt, K. R., Trauger, J. T., Watson, A. M., & Westphal, J. R. 1999, *AJ*, 118, 1657  
 Conti, P. S. 1988, in *O stars and Wolf-Rayet stars*, ed. P. S. Conti & A. B. Underhill, NASA SP-497  
 Conti, P. S. & Leep, E. M. 1974, *ApJ*, 193, 113  
 Davidson, K. & Kinman, T. D. 1982, *PASP*, 94, 634  
 D’Odorico, S. & Dopita, M. 1983, in *IAU Symp. 101: Supernova Remnants and their X-ray Emission*, ed. J. Danziger & P. Gorenstein, 517–524  
 D’Odorico, S. & Rosa, M. 1982, *A&A*, 105, 410  
 Dufton, P. L., Ryans, R. S. I., Trundle, C., Lennon, D. J., Hubeny, I., Lanz, T., & Allende Prieto, C. 2005, *A&A*, 434, 1125



- Evans, C. J., Bresolin, F., Urbaneja, M. A., Pietrzyński, G., Gieren, W., & Kudritzki, R.-P. 2007, *ApJ*, 659, 1198
- Evans, C. J. & Howarth, I. D. 2003, *MNRAS*, 345, 1223
- Evans, C. J., Howarth, I. D., Irwin, M. J., Burnley, A. W., & Harries, T. J. 2004, *MNRAS*, 353, 601
- Freedman, W. L. 1988, *AJ*, 96, 1248
- Garnett, D. R., Kennicutt, Jr., R. C., Chu, Y.-H., & Skillman, E. D. 1991, *ApJ*, 373, 458
- Georgiev, L., Borissova, J., Rosado, M., Kurtev, R., Ivanov, G., & Koenigsberger, G. 1999, *A&AS*, 134, 21
- Gieren, W., Pietrzyński, G., Bresolin, F., Kudritzki, R.-P., Minniti, D., Urbaneja, M., Soszynski, I., Storm, J., Fouque, P., Bono, G., Walker, A., & Garcia, J. 2005, *The Messenger*, 121, 23
- Hodge, P., Lee, M. G., & Gurwell, M. 1990, *PASP*, 102, 1245
- Hodge, P. W. 1978, *ApJS*, 37, 145
- Hodge, P. W., Smith, T. R., Eskridge, P. B., MacGillivray, H. T., & Beard, S. M. 1991, *ApJ*, 369, 372
- Hoffman, G. L., Salpeter, E. E., Farhat, B., Roos, T., Williams, H., & Helou, G. 1996, *ApJS*, 105, 269
- Humphreys, R. M. 1980, *ApJ*, 238, 65
- Izotov, Y. I., Stasińska, G., Meynet, G., Guseva, N. G., & Thuan, T. X. 2006, *A&A*, 448, 955
- Jaschek, M., Jaschek, C., Hubert-Delplace, A.-M., & Hubert, H. 1980, *A&AS*, 42, 103
- Kingsburgh, R. L. & Barlow, M. J. 1994, *MNRAS*, 271, 257
- . 1995, *A&A*, 295, 171
- Lake, G. & Skillman, E. D. 1989, *AJ*, 98, 1274
- Lee, H., Grebel, E. K., & Hodge, P. W. 2003, *A&A*, 401, 141
- Lennon, D. J. 1997, *A&A*, 317, 871
- Lequeux, J., Meyssonnier, N., & Azzopardi, M. 1987, *A&AS*, 67, 169
- Lozinskaya, T. A., Arkhipova, V. P., Moiseev, A. V., & Afanas'ev, V. L. 2002, *Astronomy Reports*, 46, 16
- Lozinskaya, T. A., Moiseev, A. V., & Podorvanyuk, N. Y. 2003, *Astronomy Letters*, 29, 77
- Lu, N. Y., Hoffman, G. L., Groff, T., Roos, T., & Lamphier, C. 1993, *ApJS*, 88, 383
- Maeder, A., Grebel, E. K., & Mermilliod, J.-C. 1999, *A&A*, 346, 459
- Martayan, C., Frémat, Y., Hubert, A.-M., Floquet, M., Zorec, J., & Neiner, C. 2007, *A&A*, 462, 683
- Martins, F., Schaerer, D., & Hillier, D. J. 2005, *A&A*, 436, 1049
- McConnachie, A. W. & Irwin, M. J. 2006, *MNRAS*, 365, 902
- Meaburn, J., Clayton, C. A., & Whitehead, M. J. 1988, *MNRAS*, 235, 479
- Peimbert, M., Bohigas, J., & Torres-Peimbert, S. 1988, *Revista Mexicana de Astronomia y Astrofisica*, 16, 45
- Pietrzyński, G., Gieren, W., Soszyński, I., Bresolin, F., Kudritzki, R.-P., Dall'Ora, M., Storm, J., & Bono, G. 2006, *ApJ*, 642, 216
- Puls, J., Urbaneja, M. A., Venero, R., Repolust, T., Springmann, U., Jokuthy, A., & Mokiem, M. R. 2005, *A&A*, 435, 669
- Rizzi, L., Tully, R. B., Makarov, D., Makarova, L., Dolphin, A. E., Sakai, S., & Shaya, E. J. 2007, *ArXiv Astrophysics e-prints*
- Sandage, A. 1971, *ApJ*, 166, 13
- Sandage, A. & Katem, B. 1976, *AJ*, 81, 743
- Santolaya-Rey, A. E., Puls, J., & Herrero, A. 1997, *A&A*, 323, 488
- Schlegel, D. J., Finkbeiner, D. P., & Davis, M. 1998, *ApJ*, 500, 525
- Schmidt-Kaler, T. 1982, *Landolt-Börnstein: Numerical Data and Functional Relationships in Science and Technology*, Vol. VI (K. Schaifers and H.H. Voigt (Springer-Verlag, Berlin))
- Silich, S., Lozinskaya, T., Moiseev, A., Podorvanuk, N., Rosado, M., Borissova, J., & Valdez-Gutierrez, M. 2006, *A&A*, 448, 123
- Skillman, E. D., Tolstoy, E., Cole, A. A., Dolphin, A. E., Saha, A., Gallagher, J. S., Dohm-Palmer, R. C., & Mateo, M. 2003, *ApJ*, 596, 253
- Trundle, C., Lennon, D. J., Puls, J., & Dufton, P. L. 2004, *A&A*, 417, 217
- Udalski, A., Wyrzykowski, L., Pietrzyński, G., Szewczyk, O., Szymanski, M., Kubiak, M., Soszynski, I., & Zebrun, K. 2001, *Acta Astronomica*, 51, 221
- Urbaneja, M. A., Herrero, A., Bresolin, F., Kudritzki, R.-P., Gieren, W., & Puls, J. 2003, *ApJ*, 584, L73
- Urbaneja, M. A., Herrero, A., Bresolin, F., Kudritzki, R.-P., Gieren, W., Puls, J., Przybilla, N., Najarro, F., & Pietrzyński, G. 2005, *ApJ*, 622, 862
- Valdez-Gutiérrez, M., Rosado, M., Georgiev, L., Borissova, J., & Kurtev, R. 2001, *A&A*, 366, 35
- van Dokkum, P. G. 2001, *PASP*, 113, 1420
- Walborn, N. R. 1971, *ApJS*, 23, 257
- Walborn, N. R. & Fitzpatrick, E. L. 1990, *PASP*, 102, 379
- Walborn, N. R., Lennon, D. J., Heap, S. R., Lindler, D. J., Smith, L. J., Evans, C. J., & Parker, J. W. 2000, *PASP*, 112, 1243
- Weaver, R., McCray, R., Castor, J., Shapiro, P., & Moore, R. 1977, *ApJ*, 218, 377
- Wilhelm, R., Beers, T. C., & Gray, R. O. 1999a, *AJ*, 117, 2308
- Wilhelm, R., Beers, T. C., Sommer-Larsen, J., Pier, J. R., Layden, A. C., Flynn, C., Rossi, S., & Christensen, P. R. 1999b, *AJ*, 117, 2329
- Wisniewski, J. P. & Bjorkman, K. S. 2006, *ApJ*, 652, 458